Regulation of PTEN activity by p38δ-PKD1 signaling in neutrophils confers inflammatory responses in the lung

Arne Ittner,[1] Helena Block,[3] Christoph A. Reichel,[4] Markku Varjosalo,[2] Helmuth Gehart,[1,5] Grzegorz Sumara,[1] Matthias Gstaiger,[2] Fritz Krombach,[4] Alexander Zarbock,[3] and Romeo Ricci[1,5,6]

[1]Institute of Cell Biology, [2]Institute of Systems Biology, Eidgenössische Technische Hochschule Zurich, 8006 Zurich, Switzerland
[3]Department of Anesthesiology and Critical Care Medicine, University of Münster, Max-Planck Institute Münster, 48151 Münster, Germany
[4]Walter Brendel Centre of Experimental Medicine, Ludwig-Maximilians-Universität München, 81377 Munich, Germany
[5]Institut de Génétique et de Biologie Moléculaire et Cellulaire, Institut National de la Santé et de la Recherche Médicale, Centre National de la Recherche Scientifique, Université de Strasbourg, 67404 Illkirch, France
[6]Laboratoire de Biochimie et de Biologie Moléculaire, Nouvel Hôpital Civil, Hôpitaux Universitaires de Strasbourg, Université de Strasbourg, 67091 Strasbourg, France

Despite their role in resolving inflammatory insults, neutrophils trigger inflammation-induced acute lung injury (ALI), culminating in acute respiratory distress syndrome (ARDS), a frequent complication with high mortality in humans. Molecular mechanisms underlying recruitment of neutrophils to sites of inflammation remain poorly understood. Here, we show that p38 MAP kinase p38δ is required for recruitment of neutrophils into inflammatory sites. Global and myeloid-restricted deletion of p38δ in mice results in decreased alveolar neutrophil accumulation and attenuation of ALI. p38δ counteracts the activity of its downstream target protein kinase D1 (PKD1) in neutrophils and myeloid-restricted inactivation of PKD1 leads to exacerbated lung inflammation. Importantly, p38δ and PKD1 conversely regulate PTEN activity in neutrophils, thereby controlling their extravasation and chemotaxis. PKD1 phosphorylates p85α to enhance its interaction with PTEN, leading to polarized PTEN activity, thereby regulating neutrophil migration. Thus, aberrant p38δ–PKD1 signaling in neutrophils may underlie development of ALI and life-threatening ARDS in humans.

CORRESPONDENCE
Romeo Ricci: ricci@igbmc.fr
OR
Alexander Zarbock:
zarbock@uni-muenster.de

Abbreviations used: Akt, Ak thymoma; ALI, acute lung injury; ARDS, acute respiratory distress syndrome; BH, Bcr homology; fMLP, formylmethionyl-leucyl-phenylalanine; GPCR, G protein–coupled receptor; KC, keratinocyte-derived chemokine; MAPK, mitogen-activated protein kinase; PI3K, phosphatidylinositide-3 kinase; PIP_2, phosphoinositide(4,5)phosphate; PIP_3, phosphoinositide (3,4,5)phosphate; PKD1, protein kinase D1; PLC, phospholipase C; PTEN, phosphatase and tensin homologue; SHIP-1, SH2 domain-containing inositold phosphatase 1.

Inflammatory responses in vertebrates require efficient recruitment of leukocytes (Medzhitov, 2008). Neutrophilic granulocytes particularly contribute to early inflammatory responses (Nathan, 2006). They rapidly migrate into sites of inflammation and deploy antimicrobial effectors, which inflict collateral tissue damage as they do not distinguish between host and foreign (Medzhitov, 2008). Thus, uncontrolled accumulation and activity of neutrophils can lead to profound tissue damage (Henson, 2005). This is exemplified in acute inflammatory insults of the lung, during which exacerbated neutrophil-mediated inflammation can cause acute lung injury (ALI), which eventually culminates in acute respiratory distress syndrome (ARDS; Ware and Matthay, 2000).

Neutrophils are stimulated to migrate from blood vessels to sites of inflammation by chemokines (Mackay, 2001). Sensing of chemokine gradients along the axis of polarized migrating neutrophils is mediated through heterotrimeric G protein–coupled receptors (GPCRs). Chemokine GPCRs engage a plethora of signaling pathways, including heterotrimeric G proteins and small GTPases such as RhoA and Cdc42 (Stephens et al., 2008). A key step downstream

A. Ittner's present address is the Alzheimer's and Parkinson's Disease Laboratory, Brain and Mind Research Institute, University of Sydney, Sydney, Australia.

The Rockefeller University Press $30.00
J. Exp. Med. 2012 Vol. 209 No. 12 2229-2246
www.jem.org/cgi/doi/10.1084/jem.20120677

The Journal of Experimental Medicine

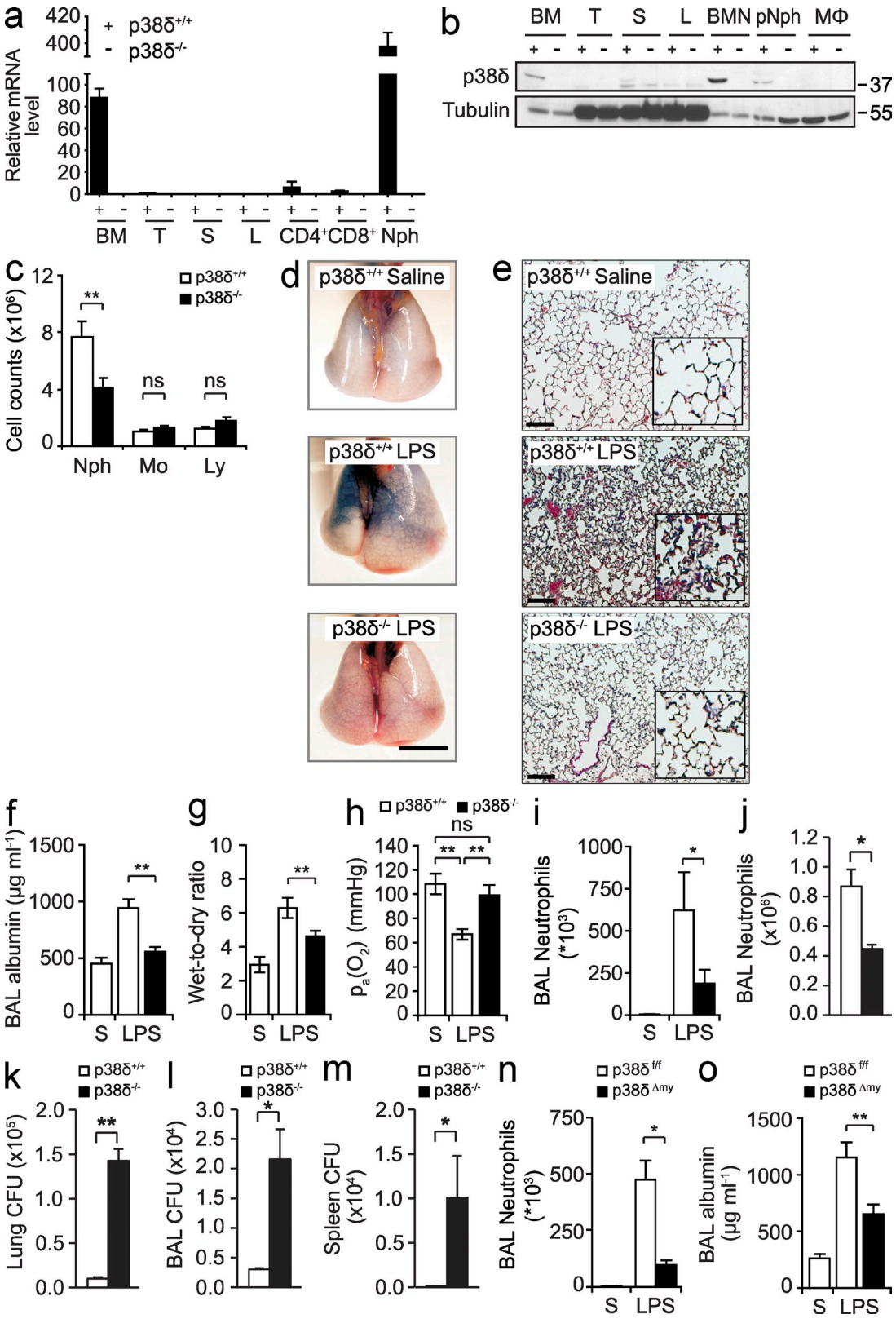

Figure 1. Deletion of *p38*δ reduces acute lung inflammation and protects mice from acute lung injury, but leads to increased bacterial burden. (a) Quantitative RT-PCR analysis of *p38*δ expression in lymphatic organs and immune cells (mean ± SD; $n = 3$). BM, total bone marrow; L, mesenteric lymph node; CD4+, CD4-positive splenocytes; CD8+, CD8-positive splenocytes; Nph, bone marrow neutrophils. (b) Expression of *p38*δ on the protein level revealed by Western blotting. BM, total bone marrow; S, spleen; T, thymus; L, mesenteric lymph node; BM-Nph, bone marrow neutrophils; pNph, peritoneal

of chemokine GPCRs is regulation of phosphoinositide-3 (PI3) kinase signaling by the G protein subunits $G_{\alpha}i/o$ and $G_{\beta\gamma}$. PI3 kinase activity at the cell front generates phosphoinositide(3,4,5)phosphate (PIP_3) from phosphoinositide(4,5) phosphate (PIP_2). This is counteracted by the activity of the PIP_3 phosphatases SH2 domain-containing inositol phosphatase 1 (SHIP-1) and phosphatase tensin homologue (PTEN) in the posterior part of the cell (Li et al., 2005; Heit et al., 2008b; Stephens et al., 2008). This system allows for rapid generation of cellular phosphoinositol phosphate gradients that are important for efficient polarization and directed migration of neutrophils. Importantly, regulation of phosphoinositide signaling is also mediated through hydrolysis of PIP_2 by phospholipase C β (PLC β) activity, which generates the second messengers diacylglycerol and inositol(1,4,5)triphosphate that activate downstream pathways such as protein kinase C, Ras, and PI3Kγ (Bunney and Katan, 2010; Suire et al., 2012).

Chemokines also activate the p38 mitogen-activated protein kinase (MAPK) cascade in neutrophils (Huang et al., 2004). Neutrophils express two p38 family members, p38α and p38δ (Hale et al., 1999; Nick et al., 1999). p38α regulates neutrophil chemotaxis mainly through its key target MAP kinase-activated kinase 2 (Huang et al., 2004). However, the specific function of p38δ in this cell type remains elusive.

Here, we specifically address the role of p38δ and its target PKD1 in neutrophil-mediated inflammation in mice. We demonstrate that p38δ inhibits PKD1 in neutrophils, thereby controlling their chemotaxis and recruitment in vivo. We also show that regulation of PKD1 activity by p38δ in neutrophils determines the degree of pulmonary tissue damage triggered by acute inflammation. Finally, we describe a distinct mechanism that directly links PLC-dependent chemokine sensing to PTEN activity through p38δ and PKD1. Thus, this study pinpoints the importance of a yet unidentified signaling pathway in neutrophil-mediated acute inflammatory processes.

RESULTS

*p38*δ is required for neutrophil recruitment to sites of inflammation and controls tissue damage and bacterial burden

We first explored the expression of p38δ in different immune compartments and cells. We confirmed high expression of p38δ in neutrophils at the mRNA and protein level (Fig. 1, a and b). Strikingly, however, p38δ was undetectable in peritoneal macrophages on both mRNA and protein levels (Fig. 1 b and not depicted). Furthermore, very low expression of p38δ was detected in spleen, thymus, and in $CD4^+$ or $CD8^+$ splenocytes (Fig. 1, a and b). This is in strong contrast to p38α, which is ubiquitously and highly expressed in all immune compartments and cells (Kumar et al., 2003). Therefore, this observation prompted us to assess the function of p38δ in neutrophils in vivo. We used sterile peritonitis in global *p38*δ knockout ($p38\delta^{-/-}$) and wild-type ($p38\delta^{+/+}$) control mice as a model of inflammation. We observed markedly reduced neutrophil recruitment to the peritoneal cavity in $p38\delta^{-/-}$ mice as compared with control $p38\delta^{+/+}$ mice. Importantly however, recruitment of macrophages and lymphocytes remained unaffected (Fig. 1 c). Blood leukocyte and bone marrow composition were similar in $p38\delta^{-/-}$ and $p38\delta^{+/+}$ mice (Table S1 and Table S2).

To study consequences of reduced neutrophil recruitment, we next used intratracheal instillation of endotoxin in mice as a widely accepted in vivo model of ALI (Matute-Bello et al., 2008). We compared lung damage in $p38\delta^{-/-}$ to $p38\delta^{+/+}$ control mice and found that $p38\delta^{-/-}$ mice were largely protected against endotoxin-induced damage and lung dysfunction. i.v. administration of Evans blue dye indicated pronounced reduction in vascular injury in $p38\delta^{-/-}$ lungs upon ALI as compared with $p38\delta^{+/+}$ lungs (Fig. 1 d). Lung histology showed considerable alveolar damage and inflammatory cell infiltration in $p38\delta^{+/+}$ mice in response to LPS. In contrast, lungs of $p38\delta^{-/-}$ mice were almost indistinguishable from saline-treated control mice (Fig. 1 e). Albumin levels in BAL fluids of $p38\delta^{-/-}$ lungs were significantly lower, indicating largely maintained vascular integrity (Fig. 1 f). Pulmonary edema formation was markedly lower in $p38\delta^{-/-}$ mice (Fig. 1 g). Remarkably, lung function assessed by arterial blood oxygen pressure was significantly impaired in $p38\delta^{+/+}$ mice but was unaltered in $p38\delta^{-/-}$ mice (Fig. 1 h). Quantification of neutrophils in BAL revealed that their alveolar accumulation was notably diminished in $p38\delta^{-/-}$ mice as compared with $p38\delta^{+/+}$ mice (Fig. 1 i). The neutrophil chemoattractants CXCL1 and CCL3 were induced to a similar extent in $p38\delta^{-/-}$ and $p38\delta^{+/+}$ lungs (unpublished data).

neutrophils; Mφ, macrophages. Tubulin was used as loading control. (c) Cell counts upon sterile peritonitis in $p38\delta^{-/-}$ and control $p38\delta^{+/+}$ mice (mean ± SEM; $n = 9$). Nph, neutrophils; Mo, Macrophages/monocytes; Ly, Lymphocytes. **, $P < 0.01$ (Student's *t* test). (d) Analysis of lung damage upon LPS-induced acute lung injury (ALI) of mice with indicated genotypes using i.v. Evans blue staining. Images of representative lung specimens are shown. Bar, 1 cm. $n = 5$. (e) Histological analysis of lungs of mice with indicated genotypes upon ALI. Representative images and magnifications in white squares are shown. Bar, 50 µm. ($n = 5$) (f) BAL albumin upon ALI in mice with indicated genotypes (mean ± SEM; $n = 8$). S, saline-treated $p38\delta^{+/+}$ controls. **, $P < 0.01$ (ANOVA). (g) Lung edema upon ALI in mice with indicated genotypes determined by wet-to-dry weight ratio of lung tissue (mean ± SEM; $n = 8$). S, saline-treated controls. **, $P < 0.01$ (ANOVA). (h) Arterial partial oxygen pressure upon ALI in mice with indicated genotypes (mean ± SEM; $n = 8$). S, saline-treated controls. **, $P < 0.01$ (ANOVA). (i) Neutrophil numbers upon ALI in BAL fluid of mice with indicated genotypes (mean ± SEM; $n = 8$). S, saline-treated controls. *, $P < 0.05$ (ANOVA). (j) Neutrophil numbers upon intratracheal infection with *E. coli* (ATCC25922) (10^6 CFU) in BAL fluid of mice with indicated genotypes at 24 h post-infection (mean ± SEM; $n = 4$). *, $P < 0.05$ (Student's *t* test). (k–m) Bacterial burden upon intratracheal infection with *E. coli* (ATCC25922) (10^6 CFU) in lung (k), BAL (l), and spleen (m) of mice with indicated genotypes at 24 h after infection (mean ± SEM; $n = 4$). **, $P < 0.01$; *, $P < 0.05$ (Student's *t* test). (n) Neutrophil numbers upon LPS-induced ALI in $p38\delta^{\Delta my}$ and $p38\delta^{f/f}$ mice in BAL fluid (mean ± SEM; $n = 8$). S, saline-treated $p38\delta^{f/f}$ control mice. *, $P < 0.05$ (ANOVA) (o) BAL albumin upon ALI in $p38\delta^{\Delta my}$ and $p38\delta^{f/f}$ mice (mean ± SEM; $n = 8$). S, saline-treated controls. **, $P < 0.01$ (ANOVA).

Lower BAL neutrophil numbers were also observed upon Gram-negative bacterial lung infection in *p38*δ$^{-/-}$ as compared with *p38*δ$^{+/+}$ lungs (Fig. 1 j). Importantly, bacterial burden was markedly higher in *p38*δ$^{-/-}$ lungs and BAL fluid (Fig. 1, k and l). Substantial splenic bacterial dissemination was only observed in *p38*δ$^{-/-}$ mice (Fig. 1 m).

To exclude contributions of p38δ in cells of nonmyeloid origin, we deleted *p38*δ specifically in the myeloid compartment by crossing floxed *p38*δ with *LysM-Cre* mice. Deletion of p38δ in neutrophils was efficient using the latter deletion approach (unpublished data). Myeloid-restricted deletion of *p38*δ (*p38*δ$^{\Delta my}$) was sufficient to reduce neutrophil recruitment to the inflamed peritoneal cavity as compared with control mice without affecting recruitment of macrophages and lymphocytes (unpublished data). Moreover, *p38*δ$^{\Delta my}$ mice showed attenuated neutrophil accumulation during ALI resulting in decreased pulmonary tissue damage (Fig. 1, n and o).

These data indicate that p38δ regulates neutrophil recruitment during lung inflammation to impact on pulmonary damage and bacterial clearance.

p38δ is required for efficient extravasation and chemotaxis of neutrophils

Defective extravasation, occurring in a multistep process, including capturing, rolling, arrest, firm adherence, and transmigration (Nathan, 2006), might underlie reduced neutrophil recruitment in mice lacking *p38*δ. We therefore quantified extravasation steps by intravital microscopy (Rossaint et al., 2011). For this purpose, we used global *p38*δ knockout mice, myeloid-specific *p38*δ knockout, bone marrow transfer from *p38*δ$^{+/+}$ or *p38*δ$^{-/-}$, as well as mixed bone marrow transfer from WT mice expressing GFP under the control of the *LysM* promoter (*LysM-GFP*) and *p38*δ$^{-/-}$ mice into C57BL/6J WT mice. Hemodynamic parameters and systemic leukocyte counts were similar between experimental groups in all intravital microscopy experiments (unpublished data).

Numbers of rolling leukocytes were similar upon stimulation with chemoattractant *N*-formylmethionyl-leucyl-phenylalanine (fMLP) in *p38*δ$^{-/-}$, *p38*δ$^{\Delta my}$ and chimeric mice as compared with control mice (data not shown). However, the number of adherent leukocytes upon stimulation with fMLP was around 50% lower in *p38*δ$^{-/-}$, in *p38*δ$^{\Delta my}$ and in chimeric mice as compared with control mice (Fig. 2 a and data not shown).

Emigration of neutrophils from the circulation requires efficient chemokine-directed transmigration across the endothelial cell layer (Nathan, 2006). The numbers of transmigrated leukocytes was significantly reduced by 70% in *p38*δ$^{-/-}$ (Fig. 2 b), in *p38*δ$^{\Delta my}$ (Fig. 2 c), in mice with single bone marrow transfers (Fig. 2, d and e) as well as mice with mixed bone marrow transfers (Fig. 2 f) as compared with corresponding control mice upon chemokine stimulation.

The reduction in transmigration is considerably higher than the one observed for cell adherence, and thus suggests that the process of migration across the endothelium itself is affected by p38δ. We therefore quantified the capacity of *p38*δ knockout neutrophils to transmigrate through endothelial cells in vitro, thereby analyzing transmigration independent of blood circulation. Transmigration of *p38*δ$^{-/-}$ neutrophils toward a chemokine across an endothelial cell layer in vitro was significantly reduced as compared with *p38*δ$^{+/+}$ cells (Fig. 2 g).

Considering the defects in transmigration of *p38*δ$^{-/-}$ neutrophils, we reasoned that p38δ might affect neutrophil chemotaxis on a single-cell level. Therefore, we used time-lapse microscopy to trace neutrophils during chemotaxis in vitro. Although *p38*δ$^{+/+}$ neutrophils readily migrated toward a gradient of fMLP, *p38*δ$^{-/-}$ cells showed a profound reduction in migration (Fig. 2 h and Videos 1 and 2). Distances covered by migrating *p38*δ$^{-/-}$ neutrophils were reduced compared with *p38*δ$^{+/+}$ cells due to lower velocity (Fig. 2, i and j). Furthermore, *p38*δ$^{-/-}$ neutrophils showed a significant aberration in directionality (Fig. 2 k). Thus, p38δ is critical for neutrophil extravasation, regulating adherence, cell motility, and directional interpretation of chemoattractant gradients.

p38δ inhibits protein kinase D1 (PKD1) to regulate neutrophil recruitment to inflamed lungs

We previously demonstrated that p38δ inhibits the activity of its target PKD1 through phosphorylation on serine 397/401 (Sumara et al., 2009). Strikingly, this regulatory mechanism seemed to also exist in neutrophils, as we found markedly enhanced activity of PKD1 in *p38*δ$^{-/-}$ neutrophils as compared with *p38*δ$^{+/+}$ cells (Fig. 3 a). PKD1, among other protein kinase C family members, is activated through PLC (Wood et al., 2005). Inhibition of PLC by the compound U73122 was sufficient to restore accumulation of neutrophils in *p38*δ$^{-/-}$ mice during sterile peritonitis (Fig. 3 b). To corroborate the importance of PKD1, we subsequently addressed the relationship between p38δ and PKD1 using conditional gene targeting in mice. We performed ALI with mice that lack *p38*δ, *PKD1* or both genes in the myeloid cell lineage (*p38*$^{\Delta my}$, *PKD1*$^{\Delta my}$ and *p38*δ *PKD1*$^{\Delta my}$ mice). Again, *p38*δ$^{\Delta my}$ mice showed mitigated lung inflammation as compared with control mice. In strong contrast, *PKD1*$^{\Delta my}$ mice displayed markedly enhanced recruitment of neutrophils and exacerbated lung injury (Fig. 3, c–e). Enhanced recruitment of neutrophils in *PKD1*$^{\Delta my}$ mice was also observed in the sterile peritonitis model (unpublished data). Importantly, *p38*δ *PKD1*$^{\Delta my}$ mice showed similarly enhanced levels of lung injury and cell recruitment as compared with *PKD1*$^{\Delta my}$ mice (Fig. 3, c–e) providing genetic evidence in vivo that PKD1 is downstream of p38δ. These results suggest that p38δ negatively regulates PKD1 signaling to modulate neutrophil recruitment in vivo.

Myeloid-restricted deletion of *PKD1* enhances neutrophil extravasation and results in uncontrolled chemotaxis

We subsequently addressed effects of PKD1 deletion in myeloid cells on steps of extravasation using mice with single and mixed bone marrow transfers for intravital microscopy. Microhemodynamic parameters and systemic leukocyte counts were comparable across the experimental groups in these experiments

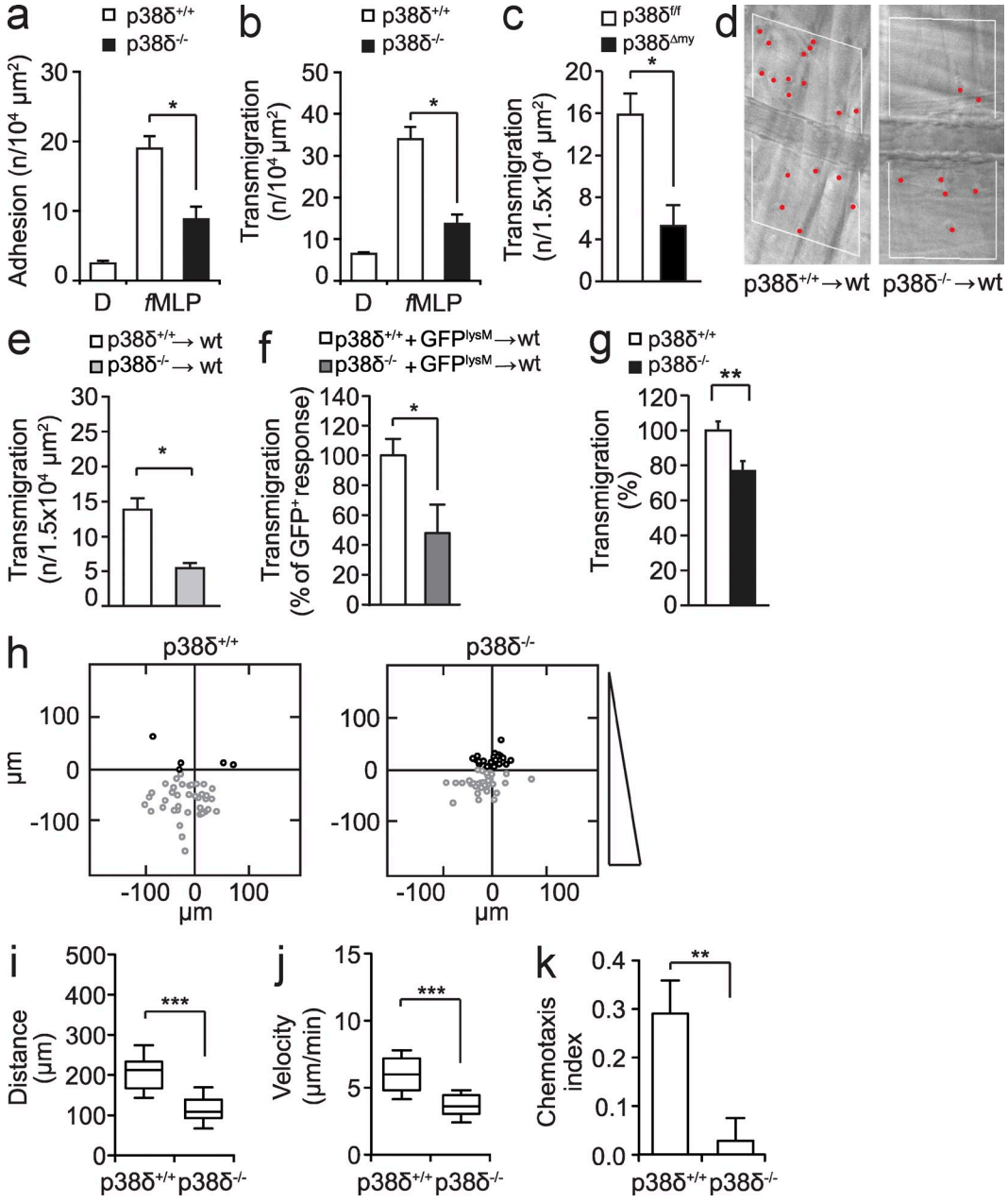

Figure 2. p38δ regulates neutrophil extravasation and chemotaxis. (a) Intravital quantification of leukocyte adhesion in muscle venules in mice with indicated genotypes after stimulation with fMLP (mean ± SEM, $n = 6$). D, DMSO-treated controls. *, $P < 0.05$. (b) Intravital leukocyte transmigration in muscle venules in mice with indicated genotypes after stimulation with fMLP (mean ± SEM; $n = 6$). D, DMSO-treated controls. *, $P < 0.05$. (c) Quantification of leukocyte transmigration by intravital microscopy in mice with indicated genotypes after stimulation with KC (mean ± SEM; $n = 3–4$). *, $P < 0.05$ (Student's *t* test). (d) Leukocyte transmigration in muscle venules of chimeric mice with indicated genotypes after KC-stimulation. Representative video stills with extravascular leukocytes in red are shown. (e) Quantification of leukocyte transmigration by intravital microscopy in single chimeric mice with indicated genotypes after stimulation with KC (mean ± SEM; $n = 3–4$). *, $P < 0.05$ (Student's *t* test). (f) Intravital leukocyte transmigration in muscle venules in mixed chimeric mice with myeloid GFP-expressing bone marrow (GFP^{lysM}) plus bone marrow of indicated genotype for *p38*δ after stimulation with KC. Data represent response of GFP-negative cells relative to the response of GFP^+ cells in the same animal. Mean ± SEM; $n = 3–4$; *, $P < 0.05$ (Student's *t* test). (g) In vitro transmigration of primary neutrophils with indicated genotypes across the endothelial cell layer (mean ± SD, $n = 5$). Values are relative to $p38\delta^{+/+}$. **, $P < 0.01$ (Student's *t* test). (h) Chemotaxis of neutrophils toward fMLP in vitro. Representative migration endpoint plots are shown for $p38\delta^{+/+}$ and $p38\delta^{-/-}$ cells. Direction of fMLP gradient is indicated. Migration distance (i) and velocity (j) from three independent experiments are expressed as box plots (mean and 10–90 percentile; $n = 50$). ***, $P < 0.001$ (Student's *t* test). (k) Chemotaxis index of neutrophils toward fMLP. Results for three independent experiments are shown (mean ± SEM; $n = 50$). **, $P < 0.01$ (Student's *t* test).

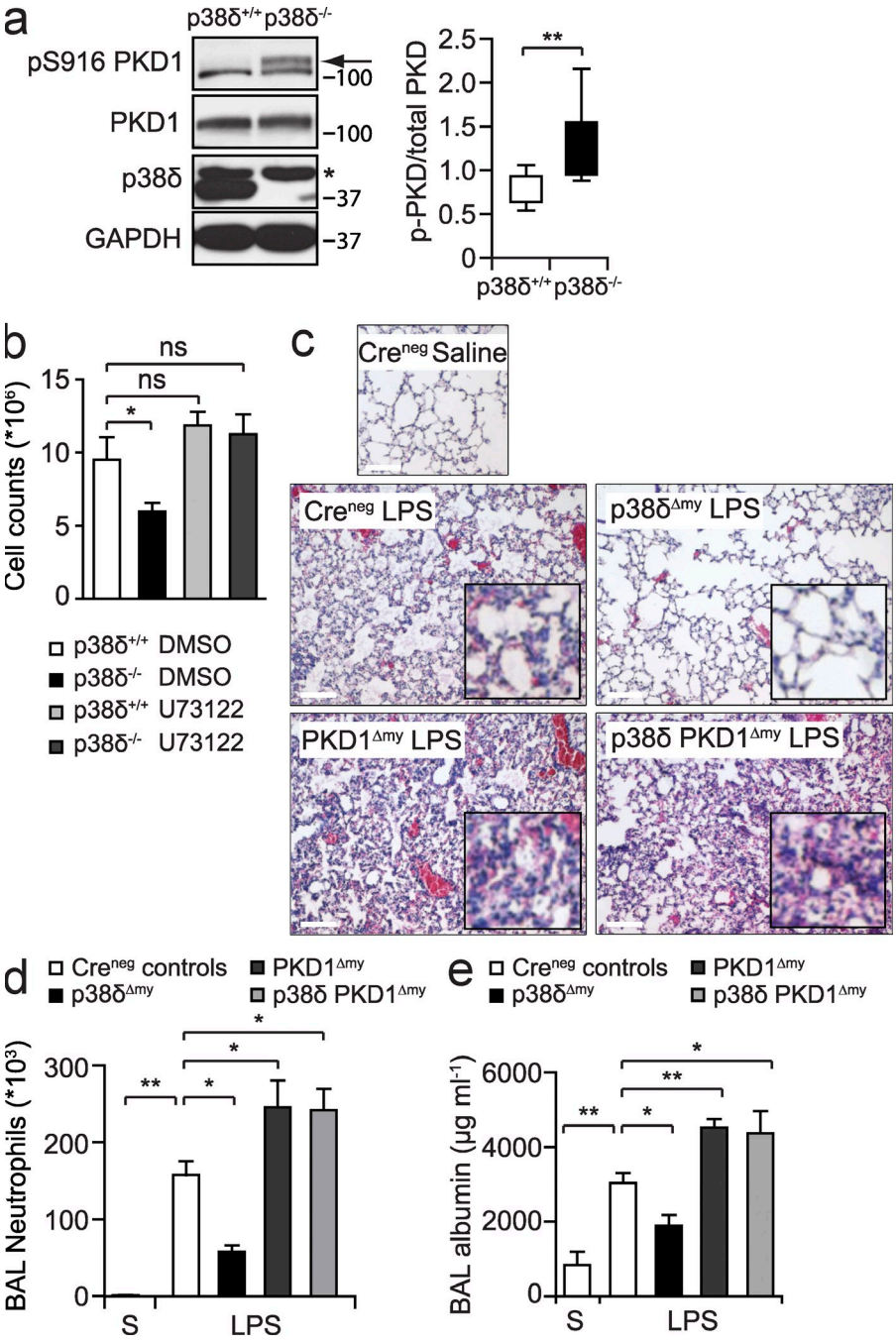

Figure 3. p38δ regulates the activity of PKD1 in neutrophils to modulate neutrophil recruitment and severity of lung injury. (a) Immunoblot with lysates from peritoneal neutrophils with indicated genotypes. Ratio of active PKD (phosphoserine916 [pS916] PKD1) to total PKD signal was determined by densitometry (mean ± SD; $n = 9$). **, $P < 0.01$ (Student's t test). (b) Sterile peritonitis with inhibition of PLC (mean ± SEM; $n = 5$). Mice with indicated genotypes were treated with DMSO or U73122. Total cell counts are shown. *, $P < 0.05$; ns, not significant (ANOVA). (c) Histological analysis of lungs of mice with the indicated genotypes during ALI. Representative images and magnifications in white squares are shown. Bars, 50 µm. (d) BAL fluid neutrophil numbers upon ALI in mice with indicated genotypes (mean ± SEM; LysMCre-negative controls (Cre^{neg}); $n = 6$ (S and LPS); $p38\delta^{\Delta my}$, $n = 3$; $PKD1^{\Delta my}$, $n = 8$; $p38\delta\ PKD1^{\Delta my}$, $n = 12$). S, saline-treated controls. **, $P < 0.01$; *, $P < 0.05$ (ANOVA). (e) BAL albumin upon ALI (mean ± SEM; LysMCre-negative controls (Cre^{neg}), $n = 6$ (S and LPS); $p38\delta^{\Delta my}$, $n = 3$; $PKD1^{\Delta my}$, $n = 8$; $p38\delta\ PKD1^{\Delta my}$, $n = 12$). S, saline-treated controls. **, $P < 0.01$; *, $P < 0.05$ (ANOVA).

(data not shown). Interestingly, leukocyte rolling flux was enhanced in chimeric as compared with control mice (Fig. 4 a and not depicted). In chimeric mice, adherent leukocyte numbers were significantly increased as compared with control mice in response to CXCL1/keratinocyte-derived chemokine (KC; Fig. 4 b and not depicted). Moreover, leukocyte transmigration was significantly elevated as compared with control mice (Fig. 4, c–e). Transmigration of $PKD1^{\Delta my}$ neutrophils toward a chemokine across an endothelial cell layer in vitro was significantly enhanced as compared with $PKD1^{f/f}$ cells (Fig. 4 f).

We then aimed at corroborating the functions of PKD1 in neutrophil chemotaxis using time-lapse microscopy. Strikingly, neutrophils isolated from $PKD1^{\Delta my}$ mice showed markedly enhanced migration in a gradient of fMLP (Fig. 4 g and Videos 3 and 4). Primary $PKD1^{\Delta my}$ neutrophils migrated with enhanced velocity (Fig. 4 h), covering larger distances (Fig. 4 i). Moreover, these cells had defective directional sensing (Fig. 4 j). These results show that PKD1 elicits opposite effects on neutrophil extravasation, adherence, and chemotaxis as compared with p38δ.

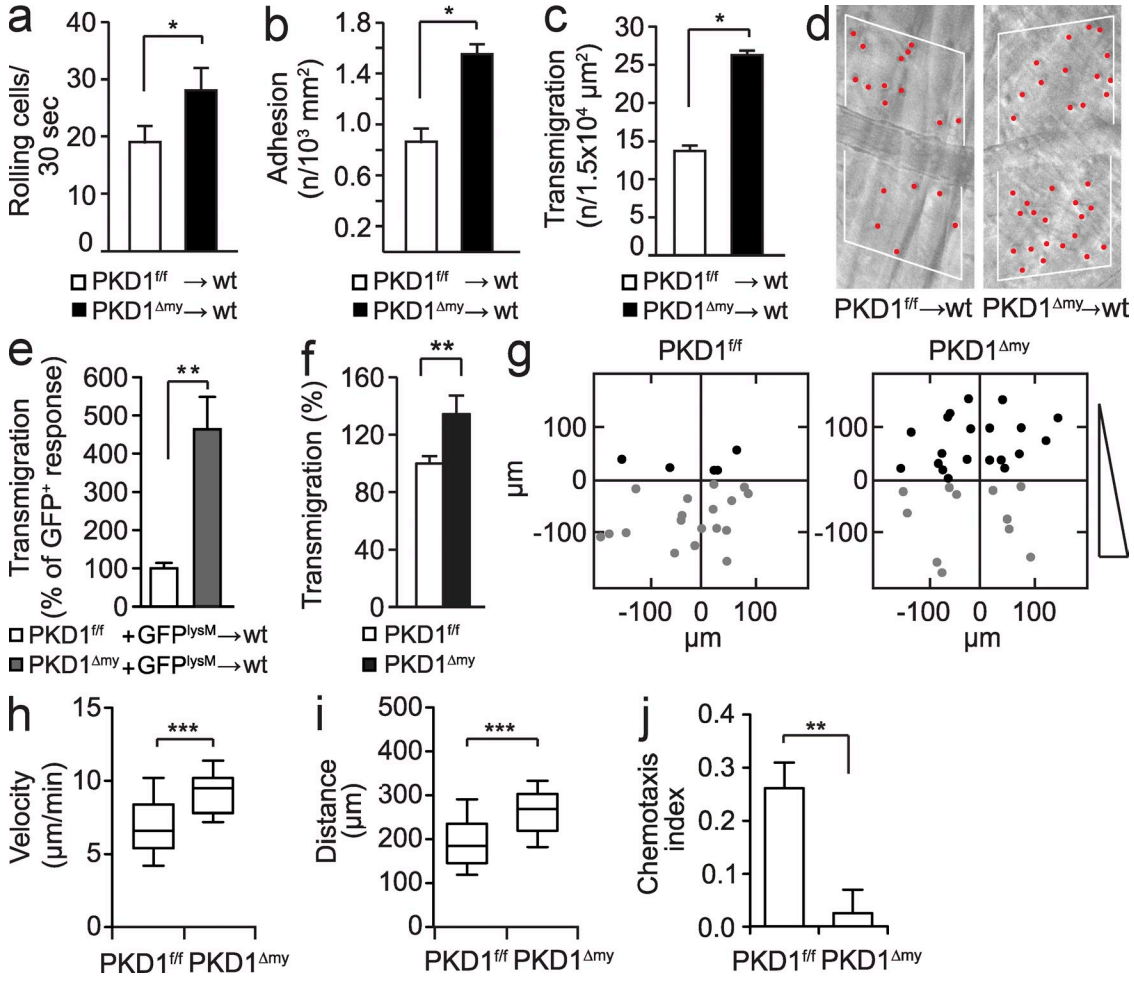

Figure 4. Deletion of *PKD1* enhances neutrophil adhesion and transmigration and alters chemotaxis. (a) Intravital quantification of leukocyte rolling in KC-stimulated muscle venules in bone marrow chimeric mice with indicated genotypes (mean ± SEM; $n = 3–4$). *, $P < 0.05$. (b) Leukocyte adhesion in KC-stimulated muscle venules in bone marrow chimeric mice with indicated genotypes (mean ± SEM; $n = 3–4$). *, $P < 0.05$. (c) Leukocyte transmigration in KC-stimulated muscle venules in bone marrow chimeric mice with indicated genotypes (mean ± SEM; $n = 3–4$). *, $P < 0.05$. (d) Intravital leukocyte transmigration in KC-stimulated muscle venules in bone marrow chimeric mice with indicated genotypes. Representative video stills with extravascular leukocytes in red are shown. (e) Intravital leukocyte transmigration in muscle venules in mixed chimeric mice with myeloid GFP-expressing bone marrow (GFP^{lysM}) plus bone marrow of indicated genotype for *PKD1* after stimulation with KC. Data represent response of GFP-negative cells relative to the response of GFP^+ cells in the same animal. Mean ± SEM; $n = 3–4$; **, $P < 0.01$; *, $P < 0.05$ (Student's *t* test). (f) In vitro transmigration of primary neutrophils with indicated genotypes across endothelial cell layer (mean ± SD; $n = 5$) Values are relative to $PKD1^{f/f}$. **, $P < 0.01$ (Student's *t* test) (g) Chemotaxis of neutrophils toward fMLP in vitro. Migration endpoint plots are shown for $PKD1^{f/f}$ and $PKD1^{\Delta my}$ cells. fMLP gradient is indicated. Velocity (h) from two independent experiments are expressed as box plots (mean and 10–90 percentile; $n = 30$). ***, $P < 0.001$ (Student's *t* test). (i) Migration distance covered by neutrophils toward fMLP in vitro. Results from two independent experiments are expressed as box plot (mean and 10–90 percentile; $n = 30$). ***, $P < 0.001$ (Student's *t* test). (j) Chemotaxis index of neutrophils toward fMLP. Results for three independent experiments are shown (mean ± SEM; $n = 30$). **, $P < 0.01$ (Student's *t* test).

p38δ and PKD1 conversely regulate PTEN function in neutrophils

Efficient directed migration of neutrophils requires polarization of signaling molecules, for example by generating a gradient of specific phosphoinositol phosphates through a localized action of PTEN and PI3K at the back and the front of the cell, respectively (Stephens et al., 2008). Interestingly, cells from myeloid-specific PTEN knockout mice showed similarly enhanced neutrophil recruitment as cells lacking PKD1 (Subramanian et al., 2007; Heit et al., 2008b; Sarraj et al., 2009). Therefore, we addressed whether PTEN abundance, subcellular distribution, and activity depended on PKD1. Immunofluorescence staining showed that localization of PTEN in $PKD1^{\Delta my}$ cells was not restricted to the uropod as seen in control $PKD1^{f/f}$ cells (Fig. 5 a). Quantification corroborated impaired PTEN localization in $PKD1^{\Delta my}$ cells as compared with control $PKD1^{f/f}$ cells (Fig. 5 b). However, polarization of F-actin to the front was similar in $PKD1^{\Delta my}$ cells and $PKD1^{f/f}$ cells (Fig. 5, a and c). Specificity of PTEN staining was confirmed using PTEN-negative PC3 cells (unpublished data).

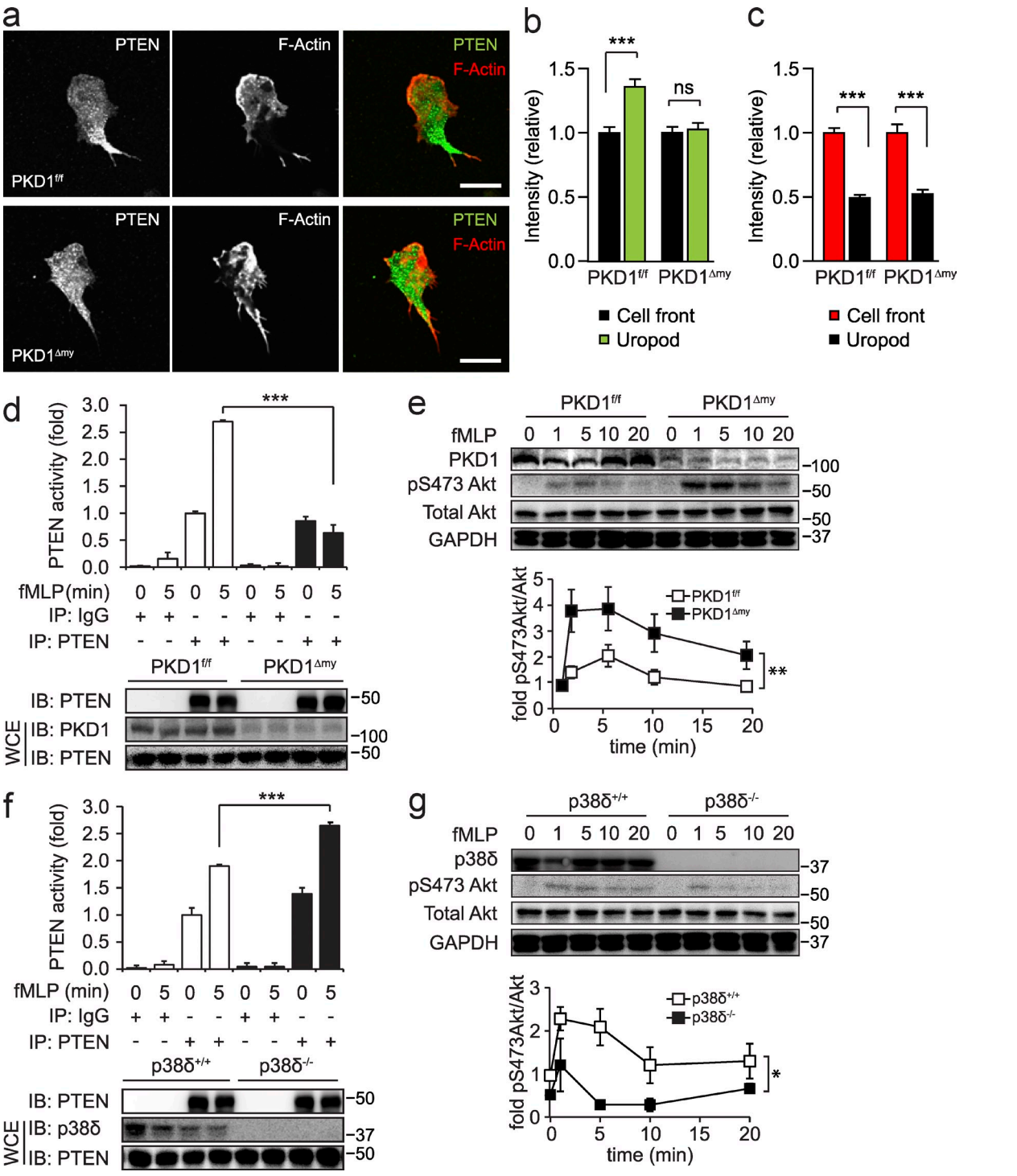

Figure 5. PKD1 regulates subcellular localization and activity of PTEN. (a) Staining of PTEN (green) and F-actin (red) in neutrophils from *PKD1*$^{f/f}$ or *PKD1*$^{\Delta my}$ mice upon stimulation with fMLP (1 µM). Representative confocal images are shown. Bars, 10 µm. (b and c) Quantification of PTEN (b) and F-actin (c) in the fronts and uropods of cells from *PKD1*$^{f/f}$ or *PKD1*$^{\Delta my}$ mice upon stimulation with fMLP (1 µM). Results from 3 independent experiments are shown ($n = 50$). ***, $P < 0.001$ (ANOVA). (d) In vitro activity of immunoprecipitated PTEN on $PI(3,4,5)P_3$ from bone marrow neutrophils from *PKD1*$^{f/f}$ or *PKD1*$^{\Delta my}$ mice upon stimulation with fMLP (1 µM). Mean ± SD; $n = 3$; **, $P < 0.01$ (ANOVA). (e) Immunoblots of primary neutrophils from *PKD1*$^{f/f}$ or *PKD1*$^{\Delta my}$ mice stimulated with fMLP (1 µM) for indicated times were probed for PKD1, phospho-serine 473 Akt, Akt, and GAPDH. Representative immunoblot and densitometric quantification are shown. Means ± SD; $n = 4$; **, $P < 0.01$ (ANOVA). (f) In vitro activity of immunoprecipitated PTEN from bone marrow neutrophils from *p38*$\delta^{+/+}$ or *p38*$\delta^{-/-}$ mice upon stimulation with fMLP (1 µM). Mean ± SD; $n = 3$; **, $P < 0.01$ (ANOVA). (g) Immunoblots of primary neutrophils from *p38*$\delta^{+/+}$ or *p38*$\delta^{-/-}$ mice stimulated with fMLP (1 µM) for indicated time were probed for p38δ, phospho-serine 473 Akt, Akt, and GAPDH. Representative immunoblot and densitometric quantification are shown. Means ± SD; $n = 4$; *, $P < 0.05$ (ANOVA).

To assess PTEN activity, we measured in vitro PIP_3 hydrolysis by PTEN immunoprecipitated from primary neutrophils. Activity of PTEN was lower in primary *PKD1*$^{\Delta my}$ neutrophils upon stimulation with fMLP as compared with control *PKD1*$^{f/f}$ cells (Fig. 5 d). Total PTEN protein levels were similar in *PKD1*$^{\Delta my}$ and *PKD1*$^{f/f}$ primary neutrophils. Phosphorylation of Akt downstream of PIP_3 formation is a key signaling event, which is inhibited by conversion of PIP_3 to PIP_2 by PTEN (Cantley, 2002). We analyzed phosphorylation of serine 473 on Akt, which serves as an indicator of upstream PI3 kinase activity and PIP_3 levels in neutrophils (Strassheim et al., 2004; Li et al., 2009; Prasad et al., 2011). Primary *PKD1*$^{\Delta my}$ neutrophils showed markedly stronger induction of Akt phosphorylation during chemokine stimulation as compared with control *PKD1*$^{f/f}$ cells (Fig. 5 e).

Neutrophils lacking p38δ show increased activity of PKD (Fig. 3 a). Thus, opposite results for PTEN and AKT activity are to be expected. Indeed, activity of immunoprecipitated PTEN was higher in *p38*δ$^{-/-}$ neutrophils upon stimulation with fMLP as compared with *p38*δ$^{+/+}$ cells (Fig. 5 f). Moreover, *p38*δ$^{-/-}$ neutrophils showed lower levels of Akt phosphorylation during chemokine stimulation as compared with *p38*δ$^{+/+}$ cells (Fig. 5 g). Collectively, these results imply that modulation of p38δ and PKD1 activity conversely regulates PTEN function in migrating neutrophils.

PKD1 regulates activity of PTEN by phosphorylation of p85α on serine 154

We next aimed at finding direct biochemical evidence for regulation of PTEN by PKD1. Therefore, we searched for novel candidate targets of PKD1 that potentially link PKD1 to PTEN. We used a specific PKD phosphorylation consensus site in an in silico screen (Table S3). This analysis revealed the product of the *pik3r1* gene p85α, which is a regulatory subunit of class I PI3 kinases (Cantley, 2002). Recent studies showed that p85α is also a positive regulator of PTEN activity (Rabinovsky et al., 2009; Chagpar et al., 2010), indicating that p85α exerts both positive and negative regulation of PI3 kinase signaling. Indeed, we found lipid phosphatase activity of PTEN markedly reduced in adherent p85α-knockdown HL60 cells as compared with nonsilencing shRNA control cells (Fig. 6 a). p85α directly binds and enhances PTEN activity through the Bcr homology (BH) domain (Chagpar et al., 2010). The BH domain contains the PKD1 consensus site at serine 154 (S154) that we identified in our in silico screen. This site is conserved throughout mammalian *pik3r1* genes (unpublished data). In an in vitro kinase assay with PKD1 and radioactively labeled ATP, recombinant p85α showed incorporation of radioactivity, which was suppressed by an inhibitor of PKD1 (Gö6976; Fig. 6 b). Phosphopeptide mapping by mass spectrometry identified S154 phosphorylation on p85α expressed in Sf9 cells, as well as other previously published phosphorylation sites (Oppermann et al., 2009). The additional S565 phosphorylation detected in the in vitro reaction may reflect an artifact, as it was not detected in Sf9 cells and does not correspond to the phosphorylation consensus site of PKD (Fig. 6 c and Table S4). We next produced recombinant human WT and mutant serine 154 to Alanine (S154A) p85α and subjected these proteins to in vitro kinase assay with PKD1. Phosphoincorporation into mutant S154A p85α was markedly reduced, confirming S154 as phosphorylation site on p85α in vitro (Fig. 6 d).

Next, we addressed whether phosphorylation of p85α affects its interaction with PTEN and the activity of PTEN. Addition of active PKD1 enhanced binding of purified HIS-p85α to recombinant GST-PTEN in vitro (Fig. 6 e). Consistently, co-transfection of active PKD1 into cells transiently expressing PTEN and p85α enhanced co-immunoprecipitation of p85α with PTEN (Fig. 6 f). Co-expression of WT p85α, S154A p85α, and phospho-mimicking p85α (S154D) with PTEN, followed by immunoprecipitation, revealed enhanced interaction of PTEN with the phospho-mimicking p85α, whereas the interaction was decreased with S154A p85α as compared with WT p85α (Fig. 6 g). Recombinant S154D p85α showed similarly enhanced binding with recombinant GST-PTEN in vitro as compared with WT p85α (unpublished data).

We then measured lipid phosphatase activity of PTEN in vitro with addition of different forms of p85α. Addition of WT p85α significantly enhanced PTEN activity as previously shown (Chagpar et al., 2010). Addition of S154D p85α significantly potentiated PTEN activity seen with addition of WT p85α, although it was significantly reduced when S154A p85α was added instead (Fig. 6 h). To confirm phosphorylation, we generated a monoclonal phospho-S154-p85α antibody. Expression of constitutive active PKD enhanced phospho-S154 signal of WT p85α, whereas kinase-dead PKD had no effect. Importantly, phospho-S154 signal was abolished when S154A p85α was expressed, indicating the specificity of the antibody (Fig. 7 a). We addressed whether phosphorylation occurs in primary neutrophils stimulated with fMLP and whether it is dependent on the presence of p38δ or PKD1. Indeed, phosphorylation of S154 p85α was induced in primary neutrophils upon chemokine-stimulation (Fig. 7, b and c). However, phosphorylation of S154 was not detected in primary neutrophils isolated from *PKD1*$^{\Delta my}$ mice (Fig. 7 b). In contrast, neutrophils from *p38*δ$^{-/-}$ mice showed enhanced phosphorylation of p85α as compared with *p38*δ$^{+/+}$ cells, which is consistent with increased PKD activity in the absence of p38δ (Fig. 7 c). Overall, these experiments suggest that PKD1-dependent phosphorylation of p85α occurs in stimulated primary neutrophils. Phosphorylation of p85α may lead to its localization in the uropod of neutrophils, where it binds and activates PTEN. Polarized colocalization of p85α and PTEN was frequently found in the uropods of *PKD1*$^{f/f}$ cells, which was much less evident in *PKD1*$^{\Delta my}$ cells. In contrast, *PKD1*$^{\Delta my}$ cells localized p85α preferentially at the front of the cell, whereas PTEN was dispersed all over the cell body (Fig. 7 d).

To address whether S154 phosphorylation of p85α is involved in chemotaxis of neutrophils, we expressed WT or mutant p85α in HL60 cells (Fig. 7 e). Live cell tracking of

transfected chemotaxing HL60 cells revealed that expression of S154A p85α enhanced migration, whereas S154D p85α expression decreased migration (Fig. 7 f and Videos 5–8), with significantly higher mean velocity of S154A p85α-expressing cells and lower velocity of S154D p85α-expressing cells (Fig. 7 g). WT p85α-expressing cells showed similar migratory behavior compared with empty vector control cells (Fig. 7, f and g). Furthermore, WT p85α-expressing cells showed

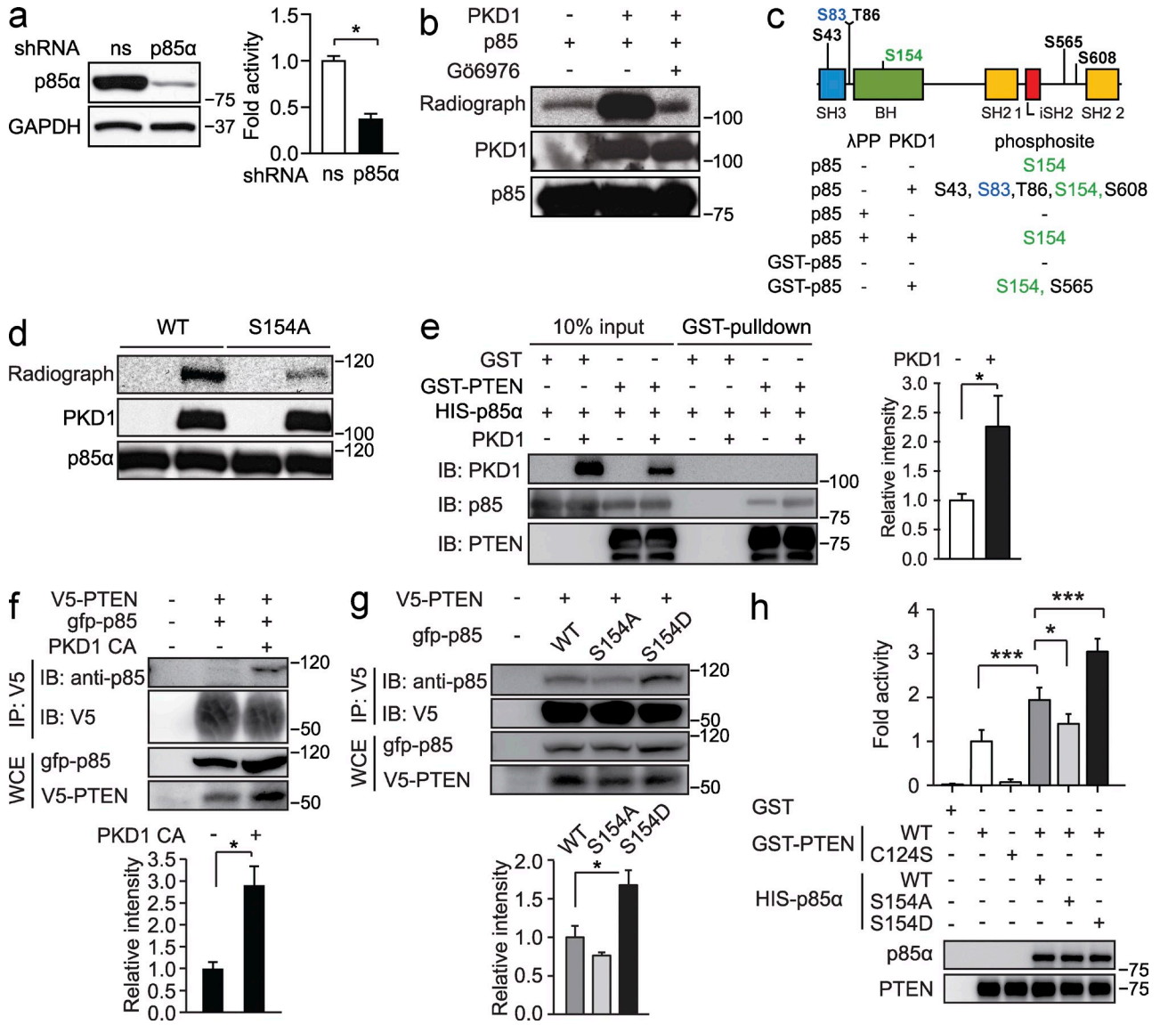

Figure 6. PKD1 phosphorylates p85α on serine 154, and phosphorylation of p85α enhances PTEN activity. (a) PTEN activity in differentiated HL-60 cells with knockdown of p85α. ns, nonsilencing. Results from two independent experiments measured in triplicate are shown as fold activity of ns. Mean ± SD; *, $P < 0.01$ (Student's *t* test). (b) In vitro kinase assay using recombinant PKD1 and p85α. Gö6976 (10 µM) was used to inhibit PKD1. (c) Phosphorylation sites in p85α from phosphopeptide mapping. SH3, src homology 3 domain; BH, Bcr homology region; SH2, src homology 2 domain; iSH2, inter-SH2. (d) In vitro kinase assay using recombinant PKD1 and recombinant nonmutated full-length GST-p85α (WT) and GST-p85α with mutation serine 154 to alanine (S154A). (e) In vitro binding assay with GST-PTEN and HIS-p85α in the presence and absence of active PKD1. Representative immunoblots for PTEN, PKD1, and p85α and densitometric quantifications are shown. Mean ± SD; $n = 3$. *, $P < 0.05$ (Student's *t* test) (f) Coimmunoprecipitation of PTEN and p85α in the presence and absence of constitutively active PKD1 (PKD1 CA, Ser738/742Glu) from whole-cell extracts [WCE] from 293T cells transiently expressing V5-PTEN, gfp-p85α, and PKD1 CA) using the indicated antibodies. Densitometric analysis (below) expressed as relative intensity to coimmunoprecipitation in absence of PKD1 CA. Mean ± SD; $n = 3$; *, $P < 0.05$ (Student's *t* test). (g) Coimmunoprecipitation of PTEN and p85α with site-specific mutations of serine 154 from WCE from 293T cells transiently expressing V5-PTEN and gfp-p85α (WT, S154A, or S154D mutants) using indicated antibodies. Densitometric analysis (below) expressed as relative intensity to gfp-p85α WT coimmunoprecipitation. Mean ± SD; $n = 4$; *, $P < 0.05$ (ANOVA) (h) In vitro PTEN activity assay using $PI(3,4,5)P_3$ as a substrate, recombinant PTEN, and p85α. PTEN activity is expressed as fold activity related to WT PTEN only (lane 2). Mean ± SD; $n = 3$; *, $P < 0.05$; ***, $P < 0.001$ (ANOVA).

transwell migration similar to that of empty vector-transfected cells, whereas cells expressing S154A p85α mutant showed higher and S154D p85α-expressing cells showed lower migratory capacity compared with WT and control cells in the same assay (Fig. 7 h). These results indicate that phosphorylation of p85α on S154 is involved in regulation of neutrophil migration.

In summary, phosphorylation of p85α on serine 154 by PKD1 increases the ability of p85α to induce PTEN activity and regulate migration (Fig. 7 i). Thus, modulation of p38δ and PKD1 activities may change PTEN activity in migrating neutrophils, altering neutrophil recruitment during acute inflammatory insults.

DISCUSSION

The degree of inflammation and associated organ damage is a result of complex pro- and antiinflammatory responses. In acute lung inflammation, this involves tight regulation of neutrophil recruitment and migration in a cell-autonomous manner. Neutrophil recruitment is governed by signals of extracellular pro- and antiinflammatory cues. Appropriate signaling in neutrophils downstream of these stimuli is thus essential to resolve inflammatory insults without causing inappropriate organ damage. We suggest that neutrophils might dynamically adapt to pro- and antiinflammatory inputs by modulating activities of p38δ and PKD1. We also provide evidence that this signaling pathway regulates PTEN, a master regulator of neutrophil recruitment. Direct regulation of PKD1 by p38δ and corresponding effects on PTEN activity allow for efficient regulation of neutrophil migration (Fig. 7 i).

A previous study identified expression of p38δ in neutrophils (Nick et al., 1999). Yet, a nonredundant function of p38δ in this cell type was not evidenced thus far. We thus provide first in vivo evidence that p38δ regulates recruitment and chemotaxis of primary neutrophils, thereby controlling pulmonary tissue injury and bacterial clearance. Because our deletion approaches in mice could not entirely exclude a potential function of p38δ in macrophages that contributed to the observed phenotypes, we performed experiments in mixed bone marrow chimeric mice to support our results with global and conditional gene deletion. p38δ-deficient neutrophils showed reduced recruitment compared with WT control cells in these mice, supporting a cell-autonomous role of p38δ in neutrophils. Furthermore, isolated p38δ-deficient neutrophils show a clear defect in chemotaxis in vitro, which is in line with reduced recruitment of neutrophils in vivo. p38δ is highly expressed in neutrophils, whereas its expression in macrophages is comparatively low. Very low expression of p38δ in macrophages as opposed to p38α has been confirmed by a recent study (Risco et al., 2012). This study also demonstrated that macrophages lacking p38δ exhibited minor changes in cytokine expression in response to LPS and that additional inactivation of p38γ was necessary to obtain more significant effects. Hence, we conclude that p38δ-dependent reduction of neutrophil recruitment in response to all tested inflammatory stimuli and mitigation of lung injury in response to LPS is likely to be independent of effects by macrophages.

Our study also provides strong experimental evidence that effects seen in p38δ-deficient mice are caused by increased PKD1 activity in neutrophils. PKD1 is expressed in both, macrophages and neutrophils. In fact, PKD1 in murine peritoneal macrophages and isolated bone-marrow–derived dendritic cells was shown to promote LPS-stimulated release of proinflammatory mediators (Park et al., 2008). Importantly, these two studies lack any data on inflammation in vivo. Using myeloid-specific deletion of PKD1, we found strikingly increased inflammatory injury in the lung in response to LPS. This observation is perfectly in line with enhanced recruitment of neutrophils to the lung and enhanced extravasation indicated by intravital microscopy in different mouse models, including mixed bone marrow chimera. In addition, the results in mixed bone marrow chimeras strongly support a cell-autonomous role of PKD1 in neutrophils rather than in other myeloid lineages. Considering a potential proinflammatory role of PKD1 in macrophages as opposed to markedly enhanced lung inflammation in myeloid-specific PKD1-null mice, we conclude that the observed effects in our study are independent of macrophages and instead largely caused by an uncontrolled influx of neutrophils.

Our results implicate PKD1 in neutrophil chemotaxis, regulating both directionality and speed of migration. *PKD1*$^{\Delta my}$ cells show enhanced cell speed, which may compensate for a defect in directionality of movement, and thus result in efficient transmigration of *PKD1*-deficient cells in vivo and in vitro. In line with this assumption, we found higher numbers of extravasated neutrophils in in vivo inflammation models in *PKD1*$^{\Delta my}$ mice. Our study is in line with studies that investigated tumor cell motility in the absence and presence of PKD1. These studies provide a mechanism that involves PKD1-mediated negative regulation of slingshot phosphatase SSH1L, which dephosphorylates and activates actin-regulator cofilin. Reduction of PKD1 led to reduced phosphorylation of cofilin and enhanced migration in fibroblasts (Eiseler et al., 2009; Peterburs et al., 2009). We did not detect differences in cofilin phosphorylation in PKD1-deficient neutrophils (unpublished data). In contrast to neutrophils, adherent cells such as fibroblasts and epithelial cells tend to form stable focal adhesions and stress fibers during migration (Stephens et al., 2008). Thus, given these differences in modes of migration, the existence of specific signaling events in different cell types is likely.

In this study, we also discovered p85α as a novel target of PKD1, providing a stunning link between PKD and PI3 kinase–PTEN signaling. p85α serves as regulatory subunit for the PI3 kinase catalytic subunits p110α, β, and δ, whereas p101 is the regulatory subunit for p110γ (Okkenhaug and Vanhaesebroeck, 2001; Vanhaesebroeck et al., 2001). Neutrophils express p110α, δ, and γ (Sadhu et al., 2003a; Condliffe et al., 2005). p110γ is responsible for initial PIP_3 accumulation at the leading edge upon chemokine stimulation (Condliffe et al., 2005; Van Keymeulen et al., 2006).

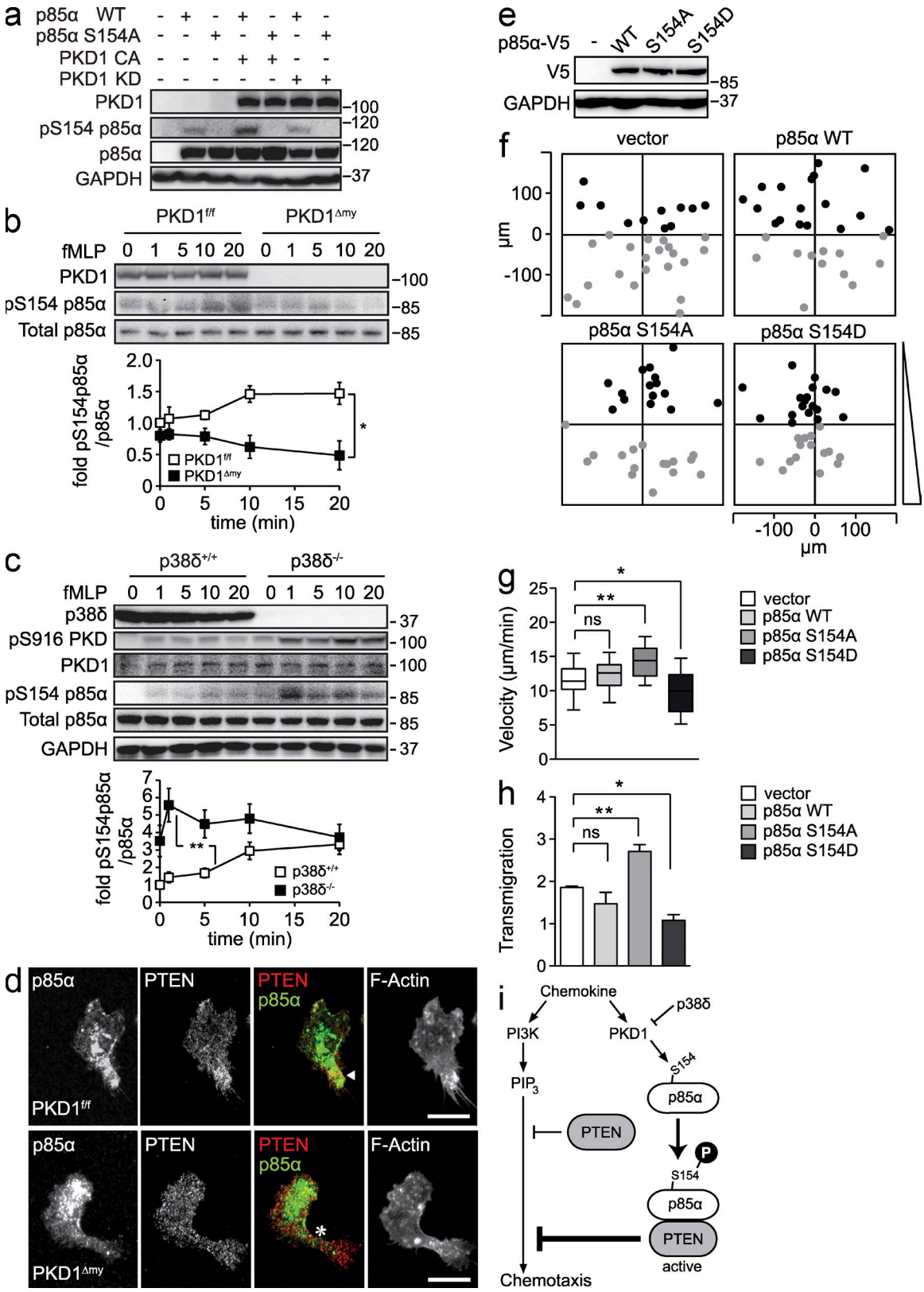

Figure 7. S154 p85α phosphorylation occurs in neutrophils in a PKD1-dependent manner and regulates migration. (a) Immunoblot of 293T cells transfected with p85α WT or S154A mutant and PKD1 constitutive active (CA) or kinase-dead (KD; K612W) were probed for PKD1, phospho-serine

Amplification of PIP_3 levels, however, depends on p110δ (Sadhu et al., 2003b; Condliffe et al., 2005). p85 has a dual function on p110; it promotes activation of PI3 kinase, but it also inhibits its activity through p85–p110 complex sequestration (Fruman et al., 1998; Vanhaesebroeck et al., 2001). Recent studies showed that p85α can also directly bind and enhance the activity of PTEN (Rabinovsky et al., 2009; Chagpar et al., 2010). Direct binding of PTEN to the BH domain of p85α promotes the activity of PTEN (Chagpar et al., 2010). We found that PKD1 phosphorylates p85α at serine 154 within the BH domain and that phosphorylation of S154 enhances binding of p85α to PTEN, and thus increases the capacity of p85α to activate PTEN. S154 phosphorylation also occurs in vivo upon chemokine stimulation of neutrophils. Overexpression of a nonphosphorylatable S154A p85α mutant was sufficient to enhance chemotaxis and migration speed of neutrophil-like HL60 cells, indicating that phosphorylation of p85α is required to control neutrophil recruitment. Overexpressing the phospho-mimicking mutant S154D p85α reduced the migratory response of HL60 cells and particularly lowered cell speed, implicating that S154 phosphorylation is an important new mechanism in migrating cells. The molecular link between PKD1, p85α, and PTEN might also be essential in other processes in which both PKD1 and PI3 kinase signaling play an essential role, including invasion and neovascularization of tumors (Di Cristofano and Pandolfi, 2000).

Our study also revealed specific localization of endogenous p85α in primary neutrophils. Localization of p85α to the back of the cell was dependent on phosphorylation by PKD1. Nonphosphorylated p85α preferentially localized to the front of the cell. PTEN cannot bind to nonphosphorylated p85α at the leading edge, but it binds specifically to phosphorylated p85α at the back of the cell. Localization of the phosphorylation site in the BH domain implies that it will not directly interfere with binding to catalytic subunits of PI3K. High affinity of PTEN to phosphorylated p85α may thus create competition with p85α binding to catalytic subunits of PI3K, specifically preventing PIP3 formation at the rear of the cell. It is, however, currently unclear how phosphorylated and nonphosphorylated p85α distinguishes the front and back of the cell. Specifically localized adaptor proteins might be necessary.

Altogether, phosphorylation of p85α results in its specific localization at the rear of the cell, leading to enrichment of PTEN and enhancement of its activity at the uropod. This may occur during the initial steps of polarization, at which point p101, and not p85α, is needed in the leading edge. Non-phosphorylated p85α localizes to the front of the cell. This may become important at later steps of polarization, when amplification of PIP3 requires p110δ, with the latter binding to p85α.

The involvement of PI3 kinase signaling in adherence is a controversial topic among researchers, which is probably a result of different experimental settings used in previous studies. p110γ-deficient neutrophils showed strongly reduced chemokine-stimulated adherence (Ferguson et al., 2007; Heit et al., 2008a). Another study found that p110γ or p110δ are dispensable for neutrophil adherence under shear stress (Puri et al., 2005). A recent study reported no changes in the adherence of neutrophils upon inhibition of PI3 kinase or deletion of PTEN in vivo (Sarraj et al., 2009). We found reduced chemokine-stimulated adherence of neutrophils in $p38\delta^{-/-}$ mice and increased adherence of $PKD1^{\Delta my}$ neutrophils in vivo using intravital microscopy. Given the possibility that neither PI3 kinase nor PTEN are essential in adherence of neutrophils under physiological shear stress, a PTEN-independent mechanism might account for the role of p38δ and PKD1 in adherence. Nevertheless, PTEN was described as a critical regulator of cell migration (Leslie et al., 2008). Spatial and temporal regulation of PTEN is involved in regulation of chemotaxis (Funamoto et al., 2002). The requirement of PTEN in chemotaxis of neutrophils in response to fMLP is controversial. In fact, migration of murine PTEN-deficient neutrophils in response to fMLP was indistinguishable from control cells, whereas granulocytes lacking the lipid phosphatase SH2 domain-containing inositol SHIP-1 showed clear defects (Nishio et al., 2007). This study thus establishes SHIP-1 as a predominant regulator of fMLP-mediated neutrophil chemotaxis. Nonetheless, occurrence of polarization of PTEN in neutrophils in response to fMLP is widely accepted (Funamoto et al., 2002), and PTEN is indeed required for chemotaxis of *Dictyostelium* (Iijima and Devreotes, 2002), an organism sharing many mechanisms of migration with neutrophils (Stephens et al., 2008). Based on these observations, investigators

154 p85α (pS154 p85α), p85α and GAPDH. ($n = 3$) (b) Immunoblots of neutrophils from $PKD1^{f/f}$ and $PKD1^{\Delta my}$ mice stimulated with fMLP (1 µM) for indicated time were probed with PKD1, phospho serine 154 p85α (pS154 p85α) and p85α. Densitometric quantifications are shown. Means ± SD; $n = 3$. *, $P < 0.05$ (ANOVA). (c) Immunoblots of neutrophils from $p38\delta^{+/+}$ or $p38\delta^{-/-}$ mice stimulated with fMLP (1 µM) for indicated time were probed for p38δ, phospho-serine 916 PKD (pS916 PKD), PKD1, pS154 p85α, and p85α. Densitometric quantifications are shown. Means ± SD; $n = 3$. **, $P < 0.01$ (ANOVA). (d) Staining of PTEN (green), p85α (red), and F-actin in neutrophils from $PKD1^{f/f}$ or $PKD1^{\Delta my}$ mice upon stimulation with fMLP (1 µM). Representative confocal images are shown. Bar, 10 µm. Arrowhead and asterisk indicate uropods. (e) Immunoblots of dHL60 cells transfected with empty vector (−) or V5-tagged p85α were probed for V5 and GAPDH. (f) Chemotaxis in response to KC/CXCL-1 (1 ng/ml) of HL-60 cells transfected with indicated constructs. Representative migration endpoint plots are shown. KC gradient is indicated. Mean migration velocity (g) from two independent experiments expressed as box plots (mean and 10–90 percentile; $n = 60$) **, $P < 0.01$; *, $P < 0.05$. ns, not significant (ANOVA). (h) Transmigration of dHL60 cells transfected with indicated constructs in transwell assay toward KC/CXCL-1 (1 ng/ml). Values are expressed as fold of unstimulated transmigration. Means ± standard error; $n = 3$) **, $P < 0.01$; *, $P < 0.05$ (ANOVA). (i) Hypothetical model of regulation of neutrophil migration by p38δ and PKD1. PKD1 is regulated by chemokines and activity of p38δ and phosphorylates p85α on serine 154. Phosphorylation enhances interaction of p85α with PTEN leading to increased activity of PTEN and lower cell motility.

continued searching for a function of PTEN in neutrophil chemotaxis. Indeed, an important subsequent study found that PTEN is not required for fMLP-induced neutrophil chemotaxis, but that it regulates migration in response to the chemokine CXCL2. By exposing neutrophils simultaneously to both chemotactic factors, thereby engaging cells to prioritize chemotactic cues, a recent study established a very precise role of PTEN in neutrophil chemotaxis (Heit et al., 2008b). The importance of these findings is highlighted by the fact, indicated by several independent research teams, that recruitment of neutrophils to sites of inflammation in vivo in mice is clearly dependent on the absence and presence of PTEN (Heit et al., 2008b; Li et al., 2009; Sarraj et al., 2009; Schabbauer et al., 2010). Hence, more recent studies established PTEN as a crucial regulator of neutrophil chemotaxis and of their recruitment to inflammatory sites in vivo (Phillipson and Kubes, 2011), confirming PTEN as a potential downstream effector of p38δ-PKD1 signaling. The question remains, however, why chemotaxis of neutrophils lacking p38δ or PKD1 is altered in response to fMLP, if their target PTEN seems not to be required for the latter process. In fact, defects in the polarization and activity of PTEN seen in our experiments are very different from the complete deletion of PTEN that was used in previous studies to investigate its requirement. Therefore, these previous experiments do not challenge our findings. In contrast, our data highlight the importance of proper PTEN localization and efficient PTEN activity in neutrophil chemotaxis to fMLP. However, our data do not exclude a complex role of p38δ and PKD1 in PTEN-dependent neutrophil chemotaxis in response to different chemotactic stimuli. This needs to be addressed further in future studies.

The leading edge of migrating cells contains high levels of PIP_3, whereas the back and sides localize PTEN and PIP_2 (Funamoto et al., 2002). PTEN was shown to bind PIP_2 within membranes, which leads to allosteric PTEN activation (Leslie et al., 2008). It was suggested that PLC acts upstream of PTEN in chemotaxing *Dictyostelium* (Kortholt et al., 2007). Mechanistically, it was proposed that PIP_2 hydrolysis by PLC regulates PTEN by creating low PIP_2 levels at the cell front (Kortholt et al., 2007). However, PIP_2 is found at much higher levels than other phosphoinositide species (Leslie et al., 2008). Because of the excess of PIP_2, specific activation of PTEN by PLC might require direct activation, in addition to binding site limitation in the membrane, in migrating cells. Indeed, our data support a direct mechanism in which PLC, through PKD1, regulates colocalization and complex formation of p85α and PTEN, and thereby PTEN activity. This mechanism is corroborated by the fact that deletion of PLCβ2/3 in neutrophils leads do similar effects in neutrophil recruitment and chemotaxis as seen in neutrophils deficient for PTEN and PKD1 (Li et al., 2000).

ALI and ARDS are characterized by strong recruitment of neutrophils to lungs in humans (Ware and Matthay, 2000). Clinically, ARDS has a poor prognosis and high mortality worldwide as there is no efficient pharmacologic therapy available that supports intensive care measures (Jain and DalNogare, 2006). Given the inverse effects on tissue injury and pathogen burden, efficient therapeutic interventions at the level of neutrophils might be difficult to achieve. Eventually, implementation of potent antimicrobials together with alteration of neutrophil recruitment through modulation of the p38δ–PKD1 signaling axis may constitute a valuable therapeutic avenue in conditions of acute inflammation including ARDS in humans.

MATERIALS AND METHODS

Mice. Mice with targeted alleles for *p38δ* (*p38δ*$^{f/f}$) and *p38δ*$^{-/-}$ mice on a C57BL/6J background were described previously (Sumara et al., 2009). To obtain *p38δ*$^{\Delta my}$ mice, *p38δ*$^{f/f}$ mice were crossed with *LysM-Cre* deleter mice (Lyz2$^{tm1(cre)Ifo}$) on a C57BL/6J background (Clausen et al., 1999). Mice with targeted alleles for *PKD1* (*PKD1*$^{f/f}$) were described previously (Fielitz et al., 2008). R. Bassel-Duby and E.N. Olson (University of Texas Southwestern, Dallas, TX) provided floxed PKD1 mice. We crossed *PKD1*$^{f/f}$ mice on a C57BL/6J background with *LysM-Cre* mice to obtain myeloid-specific PKD1 knockout mice. To obtain mice with myeloid-specific deletion of both *p38δ* and *PKD1*, *p38δ*$^{f/f}$ mice were crossed with *PKD1*$^{f/f}$ and *LysM-Cre* mice. Experiments were performed using littermate mice as controls. Mice were housed under specific pathogen–free conditions. The Swiss Federal Veterinary Office approved all animal experiments.

Antibodies and reagents. Antibody against p38δ was raised in rabbit by immunization with a peptide specific for murine p38δ (Eurogentec). Antibodies for Tubulin (Sigma-Aldrich), GAPDH, phospho-serine 916 PKD (Cell Signaling Technology), PKD (Santa Cruz Biotechnology, Inc.), FITC-labeled anti–mouse Gr1 (Ly6G/C; Miltenyi Biotec), PE-labeled anti–mouse CD11b (BioLegend), PTEN (Cell Signaling Technology), PTEN-HRP conjugate (Santa Cruz Biotechnology, Inc.), p85 (Cell Signaling Technology), phospho-serine 473 Akt (Cell Signaling Technology), phospho-Threonine 308 Akt (Cell Signaling Technology), pan-Akt (Cell Signaling Technology) are commercially available. Mouse monoclonal anti-Phospho-serine 154 p85α antibody was raised against a peptide surrounding S154 in p85α (kKGLECSTLYRTQ-pSSSNPAELRQLL) and produced using hybridoma technique. fMLP, U73122, fibronectin, fatty acid–free bovine serum albumin, Evans blue, May-Grünwald Giemsa, and Wright-Giemsa solutions were purchased from Sigma-Aldrich.

Acute lung injury. Age- and sex-matched mice were instilled intratracheally (i.t.) with 50 µg of LPS (*E. coli* LPS serotype O111:B4; Sigma-Aldrich) in 50 µl saline under anesthesia with ketamine:xylazine (80:8 mg/kg body weight). After 6 h, mice were sacrificed and lungs were lavaged with cold phosphate-buffered saline. RBCs were lysed in 0.8% NH_4Cl 0.1 mM EDTA, pH 7.4. Total cells were counted in bronchoalveolar lavage (BAL) fluids using a hemocytometer. Percentage of neutrophils of total BAL cells was determined by flow cytometry after F_c-Receptor blocking for CD11b and Gr1 with neutrophils as Gr1^{hi} CD11b^{pos} cells. Albumin was measured by ELISA (Bethyl Laboratories, Inc). Wet-to-dry weight ratio was determined with lung tissue dried at 70°C. Aortic blood oxygenation was measured on a blood gas analyzer (Bayer Diagnostics). 40 µg/g Evans blue was administered i.v., and lungs were excised after 15 min. Lungs were fixed with paraformaldehyde (PFA; 4%, pH 7.4, in PBS) under 20 mm H_2O and paraffin processed. Histological sections (5 µm) were stained with hematoxylin and eosin.

Aseptic peritonitis model. Age- and sex-matched mice were injected i.p. with 1 ml of 4% thioglycolate broth (BD). After 4 h, mice were sacrificed, and infiltrated cells were recovered in 8 ml PBS. RBCs were lysed. Total cells were counted on a hemocytometer. Ratios of neutrophils, monocytes/macrophages, and lymphocytes were distinguished by morphology on Wright-Giemsa–stained cytospins of 5×10^4 cells or, where

indicated, percentages of neutrophils and monocytes/macrophages in peritoneal infiltrates were determined by flow cytometry. Neutrophils were determined as $Gr1^{hi}$ $CD11b^{+}$ and monocytes/macrophages as $Gr1^{lo}$ $CD11b^{+}$ cells in a leukocyte scatter gate. For treatment with U73122 (Sigma-Aldrich), mice were injected i.p. with U73122 (2.5 mg/kg body weight) or vehicle (DMSO) 1 h before thioglycolate.

Bacterial lung infection. Overnight culture (37°C) of *E. coli* (American Type Culture Collection 25922) was grown in Tryptic Soy medium (Merck), and then washed and resuspended in sterile saline (0.9%) at a concentration of 2×10^7 CFU/ml. Anesthetized mice (ketamine:xylazine) were inoculated i.t. with 10^6 CFU/mouse. Initial inocula were confirmed by plating serial 10-fold dilutions on tryptic soy agar (TSA). After 24 h, CFUs were determined in BAL fluid (1 ml saline), homogenized lungs, and spleens by plating serial 10-fold dilutions on TSA. Neutrophils in BAL fluid were determined by flow cytometry for Gr1 and CD11b.

Intravital microscopy. Using near-infrared reflected light oblique transillumination in vivo microscopy (Mempel et al., 2003), leukocyte recruitment was analyzed in cremaster muscle of PBS-treated $p38\delta^{+/+}$ control mice, as well as that of $p38\delta^{+/+}$ and $p38\delta^{-/-}$ mice stimulated intrascrotally with 100 µM fMLP. Chimeric mice cremaster were stimulated by superfusion at 37°C with KC (5 nM; R&D Systems) and neutrophil recruitment was monitored 1 h after preparation of cremaster muscle (Hickey et al., 2000). Blood flow velocity was measured using intraarterial fluorescence-labeled microspheres. To assure intergroup comparability, systemic leukocyte counts, inner vessel diameter, blood flow velocity, and wall shear rate were determined. Leukocyte arrest was determined before and 1 min after i.v. injection of 600 ng CXCL1 (PeproTech), as described previously (Zarbock et al., 2007). Arrest was defined as leukocyte adhesion >30 s and expressed as cells per surface area. Surface area, S, was calculated for each vessel using $S = \pi \times d \times l_v$, where d is the diameter and l_v is the length of the vessel. Postadhesion strengthening was determined by tracking the adherent cells over time.

Isolation of primary cells. All cells were isolated from 8–12 wk old sex-matched mice. Mouse bone marrow neutrophils were isolated as previously described (Fumagalli et al., 2007). Purity of isolated cells was assessed by cytospin and by flow cytometry. Purity of isolated neutrophils was 90–95%. Cell viability (Trypan blue exclusion) was >95%. Peritoneal neutrophils were elicited by i.p. injection of thioglycolate medium and, 4 h later, peritoneal cells were recovered in complete RPMI medium (with 10% fetal calf serum and 1% penicillin/streptomycin). Peritoneal macrophages were harvested after 4 d of peritonitis in complete RPMI medium. Macrophages were enriched by differential plating. Splenocytes were enriched for $CD4^{+}$ and $CD8^{+}$ cells using a kit (Stem Cell Technologies).

In vitro chemotaxis. Chemotaxis assays were performed using peritoneal neutrophils, which show good chemotactic response (Li et al., 2000). Cells were seeded on chemotaxis µ-slides (Ibidi) coated with fibronectin (50 µg/ml) applying a gradient of fMLP (10 µM) for primary neutrophils or CXCL-1 (1ng/ml) for HL-60 cells. Time-lapse microscopy was recorded on CellR (Olympus) at 2 frames per minute for 30 min. Cells tracks were done with Manual Tracking (ImageJ) and analyzed with Chemotaxis plug-in (Ibidi) for accumulated distance and average cell velocity. Chemotaxis index is defined as overall distance migrated by cells divided by migration toward the gradient.

Cell culture. HL-60 cells (CCL-240; American Type Culture Collection) and RAW264.7 (TIB-71; American Type Culture Collection) cells were grown in complete RPMI) medium (with 10% fetal calf serum and 1% penicillin/streptomycin). Differentiation of HL-60 cells (CCL-240; American Type Culture Collection) was performed with addition of 1.5% DMSO for 4 d. RAW cells spontaneously polarized after seeding for 2 h as described (Evans and Falke, 2007). Primary murine macrophages were cultured in complete RPMI. For maintenance of puromycin resistance and shRNA, cells were cultured in presence of 3 µg/ml puromycin (Sigma-Aldrich). Cells were kept at 37°C and 5% CO_2. For transient expression and lentivirus production, 293T cells were transfected by calcium precipitation method. Lentiviral vectors encoding shRNAs against p38δ, PKD1, p85α, and nonsilencing shRNA were obtained from the MISSION shRNA library (Sigma-Aldrich). HL-60 cells were infected for 24 h with lentivirus containing pLVX with p85α cDNA C-terminally fused to V5 tag. After infection, medium was replaced for differentiation medium for 3 d.

Bone marrow transplantation. Chimeric mice and mixed chimeric mice were generated by bone marrow transplantation as described previously (Mueller et al.; Zarbock et al., 2008). In brief, bone marrow cells isolated from $p38\delta^{+/+}$, $p38\delta^{-/-}$, $PKD1^{f/f}$, $PKD1^{\Delta my}$, and/or Lys-M-GFP^{+} mice were injected i.v. into lethally irradiated C57BL/6J (wt) mice. Experiments were performed 6–8 wk after bone marrow transplantation. In mixed chimeric mice, adhesion and transmigration of both Lys-M-GFP^{+} and GFP-negative cells was determined by intravital microscopy as described above. Cell numbers were normalized to the percentage of Lys-M-GFP^{+} neutrophils in the blood. Data were expressed as adhesion and transmigration of GFP-negative cells in relation to Lys-M-GFP^{+} cells.

Bone marrow analysis and blood cell counts. Total bone marrow from femurs of mice was resuspended in Hanks' balanced salt solution (HBSS, Invitrogen). Red blood cells were lysed using lysis buffer (0.8% NH_4Cl 0.1mM EDTA pH7.4). Overall morphology was assessed on cytospins stained with Wright-Giemsa (Sigma). Bone marrow cells were double-labeled with FITC-conjugated anti-CD11b (Miltenyi Biotec) and PE-conjugated anti-Gr1 (Miltenyi Biotec) and analyzed by flow cytometry. Blood was sampled in EDTA-coated collection tubes (Sarstedt) and analyzed on a hemocytometer. Differential blood cell counts were obtained from May-Grünwald-Giemsa-stained blood smears.

Adhesion flow chamber. Adhesion flow chamber experiments were performed as described previously (Kuwano et al., 2010). In brief, protein-G precoated glass capillaries were coated with P-selectin (20 µg/ml), IL-8 (50 µg/ml), and IgG1 (15 µg/ml) or m24 (15 µg/ml) for one hour and blocked with casein (Thermo Fisher Scientific). HL60 cells were resuspended in PBS containing $MgCl_2$ and $CaCl_2$ (1 mM) with a density of 5×10^6/ml living cells. The flow chamber was perfused with the cell suspension for 2 min and rinsed with PBS (1 mM $MgCl_2$/$CaCl_2$) for 1 min. In representative images the number of cells per field of view was determined.

Quantitative RT-PCR. RNA was extracted using TRIzol (Invitrogen) and reverse transcribed using first-strand cDNA synthesis (Fermentas). Primers for p38δ and 18S rRNA were described previously(Sumara et al., 2009). Primer sequences for CXCL-1 (NM_008176) were as follows: fwd 5′-CTGGGATTCACCTCAAGAACATC-3′, rev 5′-CAGGGTCAAGGCAAGCCTC-3′, and for CCL3 (NM_011337) fwd 5′-TTCTCTGTACCATGACACTCTGC-3′, rev 5′-CGTGGAATCTTCCGGCTGTAG-3′.

Immunofluorescence. Cells were fixed with PFA for 10 min at room temperature. F-actin was stained using Phalloidin-Rhodamine (Molecular probes). Confocal microscopy was performed using LSM510-NLO (Carl Zeiss) using Zen2008 software. To quantify PTEN and F-actin polarization in neutrophils, cell front including the lamellipodium and cell back including the uropod were distinguished morphologically. The area anterior of a median between lamellipodium and uropod was defined as belonging to the cell front, whereas the area posterior of this median was defined as belonging to the uropod. ImageJ was used to determine mean fluorescence intensities within these areas and the relative intensities were calculated with respect to the cell front.

Phosphopeptide analysis by mass spectrometry. Phosphopeptides from in vitro kinase assays were identified using LC-MS^n (LTQ Orbitrap XL; Thermo Fisher Scientific), with or without enrichment by TiO_2 (Bodenmiller et al., 2007). MS/MS data were searched against UniProt

database (uniprot_sprot_human, May 18th, 2010) using Mascot (Matrix Science; Perkins et al., 1999).

PTEN activity assay. Activity of PTEN in cell lysates and of recombinant or immunoprecipitated PTEN was determined as previously described (Vemula et al., 2010).

In vitro kinase assay. In vitro kinase assays were performed as previously described (Hausser et al., 2005).

Recombinant protein purification. GST-tagged proteins were expressed in BL21DE3 cells growing in presence of ampicillin and chloramphenicol. At log phase (OD_{600} 0.6), expression was induced by addition of isopropyl-β-D-thiogalactopyranoside (IPTG; 0.1 mM) at 25°C overnight. Cells were resuspended in 15 ml NETN buffer containing protease inhibitors (Complete, Roche) and subjected to lysis by French press. Insoluble fraction was pelleted by centrifugation (12000g, 15 min, 4°C). The supernatant was mixed with 500 µl bed volume glutathione (GSH)-bound beads and orbital mixed for 3 h at 4°C. The beads were collected and washed 4 times with NETN. The GST-tagged protein was eluted with GSH (15 mM in Tris pH9) for 30 min. Polyhistidine (HIS)-tagged proteins were purified using TALON Cobalt resin (Takara Bio Inc.) according to manufacturer's description. Expression and purity of protein was determined by SDS-PAGE using Coomassie Brilliant Blue staining.

In vitro GST-PTEN binding assays. Recombinant GST-PTEN (3 µg) was incubated with recombinant HIS-p85α (6 µg) for 2 h at 4°C in GST binding buffer (20mM HEPES pH7.5, 150mM NaCl, 0.1% NP-40 Substitute, 5mM $MgCL_2$, 10% Glycerol, 2mM DTT, 1mM PMSF, Complete protease inhibitors (ROCHE). Samples were incubated on buffer-equilibrated GSH-beads, washed, and prepared for SDS-PAGE using SDS sample buffer. For binding assays, in presence of active PKD1, recombinant PKD1 (1 µg) was added to the samples together with ATP (200nM) and samples were first incubated at 25°C for 10 min.

Immunoprecipitation. Transient transfection of 293T cells was performed using phosphate precipitation method using 15 µg of plasmid DNA per 10 cm dish. Cells were lysed after 24 h in TNN Buffer (20 mM Tris, pH 7.4, 150 mM NaCl, 5 mM EDTA, 1 mM Vanadate, 10 mM NaF, 0.5 mM Pyrophosphate, Complete protease inhibitors [ROCHE]) for 20 min on ice. Lysates were centrifuged for 10 min at 11,000 *g*. Supernatants were incubated with antibodies (7 µg) overnight at 4°C. Antibody–protein complexes were precipitated with blocked Protein G beads for 2–4 h at 4°C, washed, and prepared for SDS-PAGE using SDS sample buffer.

In silico screening. In silico screening was performed using PROSITE tool (www.expasy.org) Our input consensus PKD phosphorylation site [L]-X-[R]-T-[QA]-pS with predicted phosphorylation on serine or Threonine corresponds to the sites in class II histone deacetylases, which are established PKD1 targets (Vega et al., 2004; Huynh and McKinsey, 2006; Jaggi et al., 2007). Using this consensus, our search identified a list of primary sequences, including HDACs 4, 5, 7 and phosphatidylinositol 4-kinase β, which are established targets of PKD1.

Statistical analysis. One-way ANOVA with post-tests was used for multiple groups. Student's *t* test was used for two groups. Statistical significance was considered when $P < 0.05$.

Online supplemental material. Table S1 shows that bone marrow composition in p38δ knockout mice and WT controls is comparable. Table S2 shows that basal blood parameters and leukocyte counts in whole blood of p38δ knockout mice and WT controls are comparable. Table S3 shows that an in silico screen for PKD phosphorylation consensus sites revealed several hits. Table S4 shows several phosphopeptides identified in an in vitro kinase assay by mass spectrometry. Videos S1-S8 show neutrophil migration and differntiated HL60 cell expression. Online supplemental material is available at http://www.jem.org/cgi/content/full/jem.20120677/DC1.

We thank Susann Kumpf, Julius Müller and Ivan Formentini for helping with experiments. We thank Darya Zibrova for helping for the generation of the phospho-p85α antibody. We also thank Rhonda Bassel-Duby and Eric N. Olson at University of Texas Southwestern for PKD1 floxed mice.

Studies were supported by Swiss National Science Foundation SNSF (PP0033-114856), Roche Research Foundation, Bonizzi-Theler Foundation, an ETHIIRA grant by ETH (ETH-07 09-1) and by an ERC starting grant (ERC-2011-StG, 281271-STRESSMETABOL). Experiments by the laboratory of A.Z. were supported by German Research Foundation (AZ 428/3-1, AZ 428/6-1, AZ 428/8-1 and to A.Z.) and Interdisciplinary Clinical Research Center (IZKF; Münster, Germany, to A.Z.). Experiments by the laboratory of F.K. were supported by Deutsche Forschungsgemeinschaft (DFG; RE 2885/1-1 to C.A.R) and Sonderforschungsbereich 914 of DFG to C.A.R. and F.K. We thank Huiping Jiang at Boehringer Ingelheim, USA for p38δ floxed mice. The authors declare no competing financial interests.

Author contributions: A.I. conceived experiments and conducted the majority of experiments and helped write the manuscript. H.B., C.A.R., A.Z and F.K. carried out in vivo microscopy experiments. M.V. and M.G. performed proteomic analyses. H.G. and G.S. helped with mouse experiments. A.Z. conceived of important experiments. R.R. conceived of and supervised the project and wrote the manuscript.

Submitted: 27 March 2012
Accepted: 27 September 2012

REFERENCES

Bodenmiller, B., L.N. Mueller, M. Mueller, B. Domon, and R. Aebersold. 2007. Reproducible isolation of distinct, overlapping segments of the phosphoproteome. *Nat. Methods*. 4:231–237. http://dx.doi.org/10.1038/nmeth1005

Bunney, T.D., and M. Katan. 2010. Phosphoinositide signalling in cancer: beyond PI3K and PTEN. *Nat. Rev. Cancer*. 10:342–352. http://dx.doi.org/10.1038/nrc2842

Cantley, L.C. 2002. The phosphoinositide 3-kinase pathway. *Science*. 296:1655–1657. http://dx.doi.org/10.1126/science.296.5573.1655

Chagpar, R.B., P.H. Links, M.C. Pastor, L.A. Furber, A.D. Hawrysh, M.D. Chamberlain, and D.H. Anderson. 2010. Direct positive regulation of PTEN by the p85 subunit of phosphatidylinositol 3-kinase. *Proc. Natl. Acad. Sci. USA*. 107:5471–5476. http://dx.doi.org/10.1073/pnas.0908899107

Clausen, B.E., C. Burkhardt, W. Reith, R. Renkawitz, and I. Förster. 1999. Conditional gene targeting in macrophages and granulocytes using LysMcre mice. *Transgenic Res*. 8:265–277. http://dx.doi.org/10.1023/A:1008942828960

Condliffe, A.M., K. Davidson, K.E. Anderson, C.D. Ellson, T. Crabbe, K. Okkenhaug, B. Vanhaesebroeck, M. Turner, L. Webb, M.P. Wymann, et al. 2005. Sequential activation of class IB and class IA PI3K is important for the primed respiratory burst of human but not murine neutrophils. *Blood*. 106:1432–1440. http://dx.doi.org/10.1182/blood-2005-03-0944

Di Cristofano, A., and P.P. Pandolfi. 2000. The multiple roles of PTEN in tumor suppression. *Cell*. 100:387–390. http://dx.doi.org/10.1016/S0092-8674(00)80674-1

Eiseler, T., H. Döppler, I.K. Yan, K. Kitatani, K. Mizuno, and P. Storz. 2009. Protein kinase D1 regulates cofilin-mediated F-actin reorganization and cell motility through slingshot. *Nat. Cell Biol*. 11:545–556. http://dx.doi.org/10.1038/ncb1861

Evans, J.H., and J.J. Falke. 2007. Ca2+ influx is an essential component of the positive-feedback loop that maintains leading-edge structure and activity in macrophages. *Proc. Natl. Acad. Sci. USA*. 104:16176–16181. http://dx.doi.org/10.1073/pnas.0707719104

Ferguson, G.J., L. Milne, S. Kulkarni, T. Sasaki, S. Walker, S. Andrews, T. Crabbe, P. Finan, G. Jones, S. Jackson, et al. 2007. PI(3)Kgamma has an

important context-dependent role in neutrophil chemokinesis. *Nat. Cell Biol.* 9:86–91. http://dx.doi.org/10.1038/ncb1517

Fielitz, J., M.S. Kim, J.M. Shelton, X. Qi, J.A. Hill, J.A. Richardson, R. Bassel-Duby, and E.N. Olson. 2008. Requirement of protein kinase D1 for pathological cardiac remodeling. *Proc. Natl. Acad. Sci. USA.* 105: 3059–3063. http://dx.doi.org/10.1073/pnas.0712265105

Fruman, D.A., R.E. Meyers, and L.C. Cantley. 1998. Phosphoinositide kinases. *Annu. Rev. Biochem.* 67:481–507. http://dx.doi.org/10.1146/annurev.biochem.67.1.481

Fumagalli, L., H. Zhang, A. Baruzzi, C.A. Lowell, and G. Berton. 2007. The Src family kinases Hck and Fgr regulate neutrophil responses to N-formyl-methionyl-leucyl-phenylalanine. *J. Immunol.* 178:3874–3885.

Funamoto, S., R. Meili, S. Lee, L. Parry, and R.A. Firtel. 2002. Spatial and temporal regulation of 3-phosphoinositides by PI 3-kinase and PTEN mediates chemotaxis. *Cell.* 109:611–623. http://dx.doi.org/10.1016/S0092-8674(02)00755-9

Hale, K.K., D. Trollinger, M. Rihanek, and C.L. Manthey. 1999. Differential expression and activation of p38 mitogen-activated protein kinase alpha, beta, gamma, and delta in inflammatory cell lineages. *J. Immunol.* 162:4246–4252.

Hausser, A., P. Storz, S. Märtens, G. Link, A. Toker, and K. Pfizenmaier. 2005. Protein kinase D regulates vesicular transport by phosphorylating and activating phosphatidylinositol-4 kinase IIIbeta at the Golgi complex. *Nat. Cell Biol.* 7:880–886. http://dx.doi.org/10.1038/ncb1289

Heit, B., L. Liu, P. Colarusso, K.D. Puri, and P. Kubes. 2008a. PI3K accelerates, but is not required for, neutrophil chemotaxis to fMLP. *J. Cell Sci.* 121:205–214. http://dx.doi.org/10.1242/jcs.020412

Heit, B., S.M. Robbins, C.M. Downey, Z. Guan, P. Colarusso, B.J. Miller, F.R. Jirik, and P. Kubes. 2008b. PTEN functions to 'prioritize' chemotactic cues and prevent 'distraction' in migrating neutrophils. *Nat. Immunol.* 9:743–752. http://dx.doi.org/10.1038/ni.1623

Henson, P.M. 2005. Dampening inflammation. *Nat. Immunol.* 6:1179–1181. http://dx.doi.org/10.1038/ni1205-1179

Hickey, M.J., M. Forster, D. Mitchell, J. Kaur, C. De Caigny, and P. Kubes. 2000. L-selectin facilitates emigration and extravascular locomotion of leukocytes during acute inflammatory responses in vivo. *J. Immunol.* 165:7164–7170.

Huang, C., K. Jacobson, and M.D. Schaller. 2004. MAP kinases and cell migration. *J. Cell Sci.* 117:4619–4628. http://dx.doi.org/10.1242/jcs.01481

Huynh, Q.K., and T.A. McKinsey. 2006. Protein kinase D directly phosphorylates histone deacetylase 5 via a random sequential kinetic mechanism. *Arch. Biochem. Biophys.* 450:141–148. http://dx.doi.org/10.1016/j.abb.2006.02.014

Iijima, M., and P. Devreotes. 2002. Tumor suppressor PTEN mediates sensing of chemoattractant gradients. *Cell.* 109:599–610. http://dx.doi.org/10.1016/S0092-8674(02)00745-6

Jaggi, M., C. Du, W. Zhang, and K.C. Balaji. 2007. Protein kinase D1: a protein of emerging translational interest. *Front. Biosci.* 12:3757–3767. http://dx.doi.org/10.2741/2349

Jain, R., and A. DalNogare. 2006. Pharmacological therapy for acute respiratory distress syndrome. *Mayo Clin. Proc.* 81:205–212. http://dx.doi.org/10.4065/81.2.205

Kortholt, A., J.S. King, I. Keizer-Gunnink, A.J. Harwood, and P.J. Van Haastert. 2007. Phospholipase C regulation of phosphatidylinositol 3,4,5-trisphosphate-mediated chemotaxis. *Mol. Biol. Cell.* 18:4772–4779. http://dx.doi.org/10.1091/mbc.E07-05-0407

Kumar, S., J. Boehm, and J.C. Lee. 2003. p38 MAP kinases: key signalling molecules as therapeutic targets for inflammatory diseases. *Nat. Rev. Drug Discov.* 2:717–726. http://dx.doi.org/10.1038/nrd1177

Kuwano, Y., O. Spelten, H. Zhang, K. Ley, and A. Zarbock. 2010. Rolling on E- or P-selectin induces the extended but not high-affinity conformation of LFA-1 in neutrophils. *Blood.* 116:617–624.

Leslie, N.R., I.H. Batty, H. Maccario, L. Davidson, and C.P. Downes. 2008. Understanding PTEN regulation: PIP2, polarity and protein stability. *Oncogene.* 27:5464–5476. http://dx.doi.org/10.1038/onc.2008.243

Li, Z., H. Jiang, W. Xie, Z. Zhang, A.V. Smrcka, and D. Wu. 2000. Roles of PLC-beta2 and -beta3 and PI3Kgamma in chemoattractant-mediated signal transduction. *Science.* 287:1046–1049. http://dx.doi.org/10.1126/science.287.5455.1046

Li, Z., X. Dong, Z. Wang, W. Liu, N. Deng, Y. Ding, L. Tang, T. Hla, R. Zeng, L. Li, and D. Wu. 2005. Regulation of PTEN by Rho small GTPases. *Nat. Cell Biol.* 7:399–404. http://dx.doi.org/10.1038/ncb1236

Li, Y., Y. Jia, M. Pichavant, F. Loison, B. Sarraj, A. Kasorn, J. You, B.E. Robson, D.T. Umetsu, J.P. Mizgerd, et al. 2009. Targeted deletion of tumor suppressor PTEN augments neutrophil function and enhances host defense in neutropenia-associated pneumonia. *Blood.* 113:4930–4941. http://dx.doi.org/10.1182/blood-2008-06-161414

Mackay, C.R. 2001. Chemokines: immunology's high impact factors. *Nat. Immunol.* 2:95–101. http://dx.doi.org/10.1038/84298

Matute-Bello, G., C.W. Frevert, and T.R. Martin. 2008. Animal models of acute lung injury. *Am. J. Physiol. Lung Cell. Mol. Physiol.* 295:L379–L399. http://dx.doi.org/10.1152/ajplung.00010.2008

Medzhitov, R. 2008. Origin and physiological roles of inflammation. *Nature.* 454:428–435. http://dx.doi.org/10.1038/nature07201

Mempel, T.R., C. Moser, J. Hutter, W.M. Kuebler, and F. Krombach. 2003. Visualization of leukocyte transendothelial and interstitial migration using reflected light oblique transillumination in intravital video microscopy. *J. Vasc. Res.* 40:435–441. http://dx.doi.org/10.1159/000073902

Nathan, C. 2006. Neutrophils and immunity: challenges and opportunities. *Nat. Rev. Immunol.* 6:173–182. http://dx.doi.org/10.1038/nri1785

Nick, J.A., N.J. Avdi, S.K. Young, L.A. Lehman, P.P. McDonald, S.C. Frasch, M.A. Billstrom, P.M. Henson, G.L. Johnson, and G.S. Worthen. 1999. Selective activation and functional significance of p38alpha mitogen-activated protein kinase in lipopolysaccharide-stimulated neutrophils. *J. Clin. Invest.* 103:851–858. http://dx.doi.org/10.1172/JCI5257

Nishio, M., K. Watanabe, J. Sasaki, C. Taya, S. Takasuga, R. Iizuka, T. Balla, M. Yamazaki, H. Watanabe, R. Itoh, et al. 2007. Control of cell polarity and motility by the PtdIns(3,4,5)P3 phosphatase SHIP1. *Nat. Cell Biol.* 9:36–44. http://dx.doi.org/10.1038/ncb1515

Okkenhaug, K., and B. Vanhaesebroeck. 2001. New responsibilities for the PI3K regulatory subunit p85 alpha. *Sci. STKE.* 2001:pe1. http://dx.doi.org/10.1126/stke.2001.65.pe1

Oppermann, F.S., F. Gnad, J.V. Olsen, R. Hornberger, Z. Greff, G. Kéri, M. Mann, and H. Daub. 2009. Large-scale proteomics analysis of the human kinome. *Mol. Cell. Proteomics.* 8:1751–1764. http://dx.doi.org/10.1074/mcp.M800588-MCP200

Park, J.E., Y.I. Kim, and A.K. Yi. 2008. Protein kinase D1: a new component in TLR9 signaling. *J. Immunol.* 181:2044–2055.

Perkins, D.N., D.J. Pappin, D.M. Creasy, and J.S. Cottrell. 1999. Probability-based protein identification by searching sequence databases using mass spectrometry data. *Electrophoresis.* 20:3551–3567.

Peterburs, P., J. Heering, G. Link, K. Pfizenmaier, M.A. Olayioye, and A. Hausser. 2009. Protein kinase D regulates cell migration by direct phosphorylation of the cofilin phosphatase slingshot 1 like. *Cancer Res.* 69:5634–5638. http://dx.doi.org/10.1158/0008-5472.CAN-09-0718

Phillipson, M., and P. Kubes. 2011. The neutrophil in vascular inflammation. *Nat. Med.* 17:1381–1390. http://dx.doi.org/10.1038/nm.2514

Prasad, A., Y. Jia, A. Chakraborty, Y. Li, S.K. Jain, J. Zhong, S.G. Roy, F. Loison, S. Mondal, J. Sakai, et al. 2011. Inositol hexakisphosphate kinase 1 regulates neutrophil function in innate immunity by inhibiting phosphatidylinositol-(3,4,5)-trisphosphate signaling. *Nat. Immunol.* 12:752–760. http://dx.doi.org/10.1038/ni.2052

Puri, K.D., T.A. Doggett, C.Y. Huang, J. Douangpanya, J.S. Hayflick, M. Turner, J. Penninger, and T.G. Diacovo. 2005. The role of endothelial PI3Kgamma activity in neutrophil trafficking. *Blood.* 106:150–157. http://dx.doi.org/10.1182/blood-2005-01-0023

Rabinovsky, R., P. Pochanard, C. McNear, S.M. Brachmann, J.S. Duke-Cohan, L.A. Garraway, and W.R. Sellers. 2009. p85 Associates with unphosphorylated PTEN and the PTEN-associated complex. *Mol. Cell. Biol.* 29:5377–5388. http://dx.doi.org/10.1128/MCB.01649-08

Risco, A., C. del Fresno, A. Mambol, D. Alsina-Beauchamp, K.F. MacKenzie, H.T. Yang, D.F. Barber, C. Morcelle, J.S. Arthur, S.C. Ley, et al. 2012. p38γ and p38δ kinases regulate the Toll-like receptor 4 (TLR4)-induced cytokine production by controlling ERK1/2 protein kinase pathway activation. *Proc. Natl. Acad. Sci. USA.* 109:11200–11205. http://dx.doi.org/10.1073/pnas.1207290109

Rossaint, J., O. Spelten, N. Kässens, H. Mueller, H.K. Van Aken, K. Singbartl, and A. Zarbock. 2011. Acute loss of renal function attenuates slow leukocyte rolling and transmigration by interfering with intracellular signaling. *Kidney Int.* 80:493–503. http://dx.doi.org/10.1038/ki.2011.125

Sadhu, C., K. Dick, W.T. Tino, and D.E. Staunton. 2003a. Selective role of PI3K delta in neutrophil inflammatory responses. *Biochem. Biophys. Res. Commun.* 308:764–769. http://dx.doi.org/10.1016/S0006-291X(03)01480-3

Sadhu, C., B. Masinovsky, K. Dick, C.G. Sowell, and D.E. Staunton. 2003b. Essential role of phosphoinositide 3-kinase delta in neutrophil directional movement. *J. Immunol.* 170:2647–2654.

Sarraj, B., S. Massberg, Y. Li, A. Kasorn, K. Subramanian, F. Loison, L.E. Silberstein, U. von Andrian, and H.R. Luo. 2009. Myeloid-specific deletion of tumor suppressor PTEN augments neutrophil transendothelial migration during inflammation. *J. Immunol.* 182:7190–7200. http://dx.doi.org/10.4049/jimmunol.0802562

Schabbauer, G., U. Matt, P. Günzl, J. Warszawska, T. Furtner, E. Hainzl, I. Elbau, I. Mesteri, B. Doninger, B.R. Binder, and S. Knapp. 2010. Myeloid PTEN promotes inflammation but impairs bactericidal activities during murine pneumococcal pneumonia. *J. Immunol.* 185:468–476. http://dx.doi.org/10.4049/jimmunol.0902221

Stephens, L., L. Milne, and P. Hawkins. 2008. Moving towards a better understanding of chemotaxis. *Curr. Biol.* 18:R485–R494. http://dx.doi.org/10.1016/j.cub.2008.04.048

Strassheim, D., K. Asehnoune, J.S. Park, J.Y. Kim, Q. He, D. Richter, K. Kuhn, S. Mitra, and E. Abraham. 2004. Phosphoinositide 3-kinase and Akt occupy central roles in inflammatory responses of Toll-like receptor 2-stimulated neutrophils. *J. Immunol.* 172:5727–5733.

Subramanian, K.K., Y. Jia, D. Zhu, B.T. Simms, H. Jo, H. Hattori, J. You, J.P. Mizgerd, and H.R. Luo. 2007. Tumor suppressor PTEN is a physiologic suppressor of chemoattractant-mediated neutrophil functions. *Blood.* 109:4028–4037. http://dx.doi.org/10.1182/blood-2006-10-055319

Suire, S., C. Lécureuil, K.E. Anderson, G. Damoulakis, I. Niewczas, K. Davidson, H. Guillou, D. Pan, Jonathan Clark, Phillip T. Hawkins, and L. Stephens. 2012. GPCR activation of Ras and PI3Kc in neutrophils depends on PLCb2/b3 and the RasGEF RasGRP4. *EMBO J.* 31:3118–3129. http://dx.doi.org/10.1038/emboj.2012.167

Sumara, G., I. Formentini, S. Collins, I. Sumara, R. Windak, B. Bodenmiller, R. Ramracheya, D. Caille, H. Jiang, K.A. Platt, et al. 2009. Regulation of PKD by the MAPK p38delta in insulin secretion and glucose homeostasis. *Cell.* 136:235–248. http://dx.doi.org/10.1016/j.cell.2008.11.018

Van Keymeulen, A., K. Wong, Z.A. Knight, C. Govaerts, K.M. Hahn, K.M. Shokat, and H.R. Bourne. 2006. To stabilize neutrophil polarity, PIP3 and Cdc42 augment RhoA activity at the back as well as signals at the front. *J. Cell Biol.* 174:437–445. http://dx.doi.org/10.1083/jcb.200604113

Vanhaesebroeck, B., S.J. Leevers, K. Ahmadi, J. Timms, R. Katso, P.C. Driscoll, R. Woscholski, P.J. Parker, and M.D. Waterfield. 2001. Synthesis and function of 3-phosphorylated inositol lipids. *Annu. Rev. Biochem.* 70:535–602. http://dx.doi.org/10.1146/annurev.biochem.70.1.535

Vega, R.B., B.C. Harrison, E. Meadows, C.R. Roberts, P.J. Papst, E.N. Olson, and T.A. McKinsey. 2004. Protein kinases C and D mediate agonist-dependent cardiac hypertrophy through nuclear export of histone deacetylase 5. *Mol. Cell. Biol.* 24:8374–8385. http://dx.doi.org/10.1128/MCB.24.19.8374-8385.2004

Vemula, S., J. Shi, P. Hanneman, L. Wei, and R. Kapur. 2010. ROCK1 functions as a suppressor of inflammatory cell migration by regulating PTEN phosphorylation and stability. *Blood.* 115:1785–1796. http://dx.doi.org/10.1182/blood-2009-08-237222

Ware, L.B., and M.A. Matthay. 2000. The acute respiratory distress syndrome. *N. Engl. J. Med.* 342:1334–1349. http://dx.doi.org/10.1056/NEJM200005043421806

Wood, C.D., U. Marklund, and D.A. Cantrell. 2005. Dual phospholipase C/diacylglycerol requirement for protein kinase D1 activation in lymphocytes. *J. Biol. Chem.* 280:6245–6251. http://dx.doi.org/10.1074/jbc.M411564200

Zarbock, A., T.L. Deem, T.L. Burcin, and K. Ley. 2007. Galphai2 is required for chemokine-induced neutrophil arrest. *Blood.* 110:3773–3779. http://dx.doi.org/10.1182/blood-2007-06-094565

Zarbock, A., C.L. Abram, M. Hundt, A. Altman, C.A. Lowell, and K. Ley. 2008. PSGL-1 engagement by E-selectin signals through Src kinase Fgr and ITAM adapters DAP12 and FcR gamma to induce slow leukocyte rolling. *J. Exp. Med.* 205:2339–2347. http://dx.doi.org/10.1084/jem.20072660